The potential role of human immune cells in the systemic dissemination of enterovirus-D68

Short title: Role of human immune cells in enterovirus-D68 systemic dissemination

Brigitta M. Laksono[1,*], Syriam Sooksawasdi Na Ayudhya[1,*], Muriel Aguilar-Bretones[1], Carmen W. E. Embregts[1], Gijsbert P van Nierop[1] , Debby van Riel[1,#]

[1]Department of Viroscience, Erasmus MC, Rotterdam, South Holland, the Netherlands

*Authors contributed equally; order was determined alphabetically

#Correspondence to:

Dr Debby van Riel (d.vanriel@erasmusmc.nl)

Department of Viroscience, Erasmus MC

Dr Molewaterplein 40, 3015 GD, Rotterdam, South Holland, the Netherlands

Abstract (216/300 words)

Enterovirus-D68 (EV-D68) often causes mild respiratory infections, but can also cause severe respiratory infections and extra-respiratory complications, including acute flaccid myelitis (AFM). Systemic dissemination of EV-D68 is crucial for the development of extra-respiratory diseases, but it is currently unclear how EV-D68 viremia occurs. We hypothesize that immune cells contribute to the systemic dissemination of EV-D68, as this is a mechanism commonly used by other enteroviruses. Therefore, we investigated the susceptibility and permissiveness of human primary immune cells for different EV-D68 isolates. In human peripheral blood mononuclear cells (PBMC) inoculated with EV-D68, only B cells were susceptible but virus replication was limited. However, B cell-rich cultures, such as Epstein-Barr virus-transformed B-lymphoblastoid cell line (BLCL) and primary lentivirus-transduced B cells, were productively infected. In BLCL, neuraminidase treatment to remove α2,6- and α2,3-linked sialic acids resulted in a significant decrease of EV-D68 infected cells, suggesting that sialic acids are the functional receptor on B cells. Subsequently, we showed that dendritic cells (DCs), particularly immature DCs, are susceptible and permissive for EV-D68 infection and that they can spread EV-D68 to autologous BLCL. Altogether, our findings suggest that immune cells, especially B cells and DCs, play an important role in the development the systemic dissemination of EV-D68 during an infection, which is an essential step towards the development of extra-respiratory complications.

Author summary (195/200 words)

Enterovirus D68 (EV-D68) is an emerging respiratory virus that has caused outbreaks worldwide since 2014. EV-D68 infects primarily respiratory epithelial cells and the infection commonly results in mild respiratory diseases. However, EV-D68 infection is also associated with complications outside the respiratory tract, including a polio-like paralysis. Despite the severity of these extra-respiratory complications, it is unclear how EV-D68 is able to spread outside the respiratory tract and infect other organs, like the central nervous system (CNS). To understand this, we investigated if immune cells play a role in the extra-respiratory spread of EV-D68. We showed that EV-D68 can infect and replicate in specific immune cells, *i.e.* B cells and dendritic cells (DCs), and that the virus can be transferred from DCs to B cells. Our findings suggest that lymphoid tissues, which harbor many immune cells, can be a secondary replication site for EV-D68, from where virus is released in the circulation. Our data reveal the importance of immune cells in the systemic spread of EV-D68, which is essential for infection of extra-respiratory tissues. Intervention strategies that prevent EV-D68 infection of immune cells will therefore potentially prevent virus spread from the respiratory tract to other organs.

Introduction

Enterovirus D68 (EV-D68) is a small non-enveloped, positive single-stranded RNA virus that belongs to the family *Picornaviridae*, genus *Enterovirus.* Although EV-D68 causes predominantly mild upper respiratory tract symptoms, EV-D68 caused outbreaks of severe respiratory diseases worldwide in 2014, which were associated with neurological complications in some individuals. Among these complications, acute flaccid myelitis (AFM) was most frequently reported (1-4). Since then, EV-D68 has caused biennial outbreaks of severe respiratory disease and AFM up to 2018 (3, 5). EV-D68 circulation was limited during the pandemic, partly due to COVID-19 measures, but EV-D68-associated severe respiratory illnesses have been rising in several countries since 2021 and 2022 due to easing of COVID-19 measures (6, 7). Throughout the years, multiple clades of EV-D68 circulated, but so far there is little evidence for differences in the virulence of these viruses (1, 8, 9).

The ability of EV-D68 to disseminate into the circulation (viremia) is essential for the virus to spread from the respiratory tract, which is the primary replication site of the virus, to other organs, such as the central nervous system (CNS), and cause extra-respiratory complications. However, despite the importance of viremia in the pathogenesis of EV-D68 infection, the mechanism that leads to EV-D68 viremia is poorly understood.

Studies in mice, ferrets and patient samples have shown that the virus or viral RNA can be detected in the circulation and extra-respiratory tissues (1, 10-17). In intranasally inoculated mice, virus was detected in the blood within 24 hours post-inoculation (hpi), and in extra-respiratory tissues, such as the spleen and skeletal muscles (10, 11). In intranasally inoculated ferrets, virus was detected in axillary lymph nodes at multiple days post-inoculation (earliest detection at day 5 post-inoculation) (12). In humans, virus and viral RNA have been detected in serum of EV-D68 patients, but it is currently unknown how frequent viremia occurs during an EV-D68 infection (13-17). In addition, it is unclear whether the virus detected in the circulation is a direct spill-over from the respiratory tract or whether virus first spreads to and replicates in other tissues, *e.g.* lymphoid tissues, before disseminating into the circulation.

Other EVs, such as poliovirus and EV-A71, are known to replicate in lymphoid tissues, resulting in a sustained production of infectious viruses and subsequent spill-over into the circulation (18-22). In the case of EV-D68, the role of immune cells and lymphoid tissues in the development of viremia remains unclear. Previous studies have shown that EV-D68 productively infects several human immune cell lines, such as granulocytic (KG-1), monocytic

(U-937), T (Jurkat and MOLT) and B (Raji) cell lines (23), suggesting that immune cells or lymphoid tissues may play a role in the development of EV-D68 viremia. Here, we investigated the susceptibility and permissiveness of human primary immune cells to infection of EV-D68 from different clades to unravel the potential role of immune cells in the development of viremia and to investigate if there are clade-specific differences in the susceptibility and permissiveness of these cells. Subsequently, we investigated whether dendritic cells (DCs) can transmit virus to other immune cells, such as B cells.

Results

Human B cells are susceptible and permissive to EV-D68 infection

To investigate whether human leukocyte subsets are susceptible to EV-D68 infection, human peripheral blood mononuclear cells (PBMC) were inoculated with EV-D68 strains from subclades A, B2 and D. We observed that B cells were susceptible to infection with EV-D68/A (mean 6% ± standard error of mean (SEM) 1) and EV-D68/B2 (3% ± 1) but not for EV-D68/D, based on intracellular expression of EV-D68 capsid protein VP1. In one donor, 3% of monocytes were susceptible to infection with EV-D68/A. We did not observe any $VP1^+$ cells in $CD4^+$ nor $CD8^+$ T cell population. (**Fig 1A**).

Next, we investigated whether EV-D68 inoculation of PBMC resulted in a productive infection. Supernatant and cell lysate were collected and the presence of infectious virus particles at 0, 6, 8, 10, 24, 48 and 72 hpi was determined by virus titration. Despite the presence of infected cells after inoculation with EV-D68/A or EV-D68/B2, we did not observe an increase in infectious virus titer at any time point (**Fig 1B**). As human PBMC consists only of 4 – 14% of B cells, (24) of which 3 – 6% were infected by EV-D68, we cannot exclude the possibility that viral replication occurs in $VP1^+$ B cells but this was below the detection limit of the assay.

In order to determine whether B cells are susceptible and permissive for EV-D68, we utilized two B cell-rich models. We first inoculated Epstein-Barr virus-transformed B-lymphoblastoid cell line (BLCL) with EV-D68 strains from subclades A, B2 and D. The inoculation resulted in 13% ± 4 EV-D68/A, 18% ± 5 EV-D68/B2 and 21% ± 4 EV-D68/D $VP1^+$ cells, although there was variation among donors in the percentage of infected cells (**Fig 2A**). Production of new infectious viruses over time (~2 – 3 logarithmic increase of $TCID_{50}$/ml within 24 hours) was detected after inoculation with all three viruses, in which EV-D68/B2 and EV-D68/D replicated faster than EV-D68/A, albeit without any statistical differences (**Fig 2B**).

Primary B cell clones that were lentivirus-transduced to express the germinal center-associated B cell lymphoma-6 (Bcl-6) and Bcl-xL in order to endow a stable proliferative state, were inoculated with EV-D68 strains from subclades A, B2 and D. This resulted in 11% ± 2 EV-D68/A, 27% ± 8 EV-D68/B2 and 14% ± 6 EV-D68/D $VP1^+$ cells (**Fig 2C)**. The inoculation also resulted in production of new infectious viruses (~2 – 3 logarithmic increase within 10 to 24 hours), without any statistical differences among the different EV-D68 clades **(Fig 2D)**.

Infection of BLCL is largely mediated by the presence of α2,3- and α2,6-linked SAs

Several immune cells, including B cells, express α2,6-linked and α2,3-linked sialic acids (SAs), which can function as receptors for EV-D68 to initiate binding and virus entry (25-27). To investigate whether α2,3- and α2,6-linked SAs mediate EV-D68 infection of BLCL, BLCL were treated with *Arthrobacter ureafaciens* neuraminidase (ANA) to remove cell surface SAs prior to inoculation with EV-D68 strains. Upon ANA treatment, the average percentages of α2,3-linked SA^+ BLCL decreased from 77% ± 9 to 38% ± 3 and of α2,6-linked SA^+ cells from 89% ± 1 to 5% ± 1 (**Fig 3A**). ANA treatment of BLCL prior to inoculation resulted in a significant decrease of percentage of $VP1^+$ cells, with only 2% ± 1 EV-D68/A, 5% ± 2 EV-D68/B2 and 5% ± 1 EV-D68/D $VP1^+$ cells (**Fig 3B**).

Dendritic cells (DCs) are susceptible and permissive to EV-D68 infection

DCs are a subset of immune cells that are attracted to sites of inflammation, but not abundantly present in PBMC (28). To investigate whether DCs are susceptible and permissive to EV-D68 infection, monocytes were differentiated in immature and mature DCs (imDCs and mDCs, respectively), and inoculated with EV-D68 strain from subclade A as a representative strain. Increased expression of maturation markers (HLA-DR, CD86, PD-L1 and CD83) was used to confirm differentiation of imDCs to mDCs (**S1 Fig)**. The average percentage of $VP1^+$ cells in imDCs (10% ± 1) was significantly higher than in mDCs (4% ± 1) at 6 hpi (**Fig 4A**). From 2 to 10 hpi, viral titers in the supernatants increased ~1 logarithmic $TCID_{50}$/ml in imDCs and ~0.5 logarithmic $TCID_{50}$/ml in mDCs inoculated with EV-D68/A, after which the virus titers decreased. Despite this decrease, at 48 hpi, virus titer in the supernatants of imDCs were significantly higher than in mDCs (**Fig 4B**).

imDCs can tranfer EV-D68 to autologous BLCL

Dendritic cells are important for local antiviral responses and antigen take-up induces DC maturation and migration to lymphoid tissues (28). Therefore, we investigated whether imDCs can transmit EV-D68 infection to B cells. EV-D68/A-inoculated imDCs were co-cultured with autologous BLCL (BLCL+DC), after which the percentages of $VP1^+$ BLCLs were determined. The following controls were included: (1) EV-D68/A-inoculated imDCs (DC only); (2) BLCL cultured with supernatant from EV-D68/A-inoculated imDCs collected at 0 hpi, directly after the virus inoculation for 1 hour and the subsequent washing steps (BLCL + t0 DC sup) and (3) BLCL cultured with supernatant from EV-D68/A-inoculated imDCs collected at 6 hpi (BLCL + t6 DC sup). The

schematic representation of this experiment is presented in **Fig 5A.** As observed previously, inoculation of imDCs in the absence of their autologous BLCL resulted in an average of 11% ± 2 $VP1^+$ cells at 6 hpi and the percentage remained stable at 24 hpi. In imDCs co-cultured with BLCL, we observed an average percentage of 10% ± 4 $VP1^+$ imDCs, although this percentage decreased at 24 hpi (4% ± 2) (**Fig 5B**). When BLCLs were inoculated with supernatants from EV-D68-inoculated imDCs collected at 0 or 6 hpi, only very few B cells were infected, with average percentages of 0.5% $VP1^+$ BLCLs in BLCL+t0 DC sup and 1% $VP1^+$ BLCLs in BLCL+t6 DC sup at 24 hpi. When BLCLs were co-cultured with EV-D68-inoculated imDCs, the percentage of infected BLCL increased from 2%±1 at 6 hpi to 6% ± 1 at 24 hpi (**Fig 5C**).

The inoculation of imDCs in the absence of BLCL resulted in production of new infectious virus particles (~1.5 logarithmic increase of $TCID_{50}$/ml) within 24 h. Detection of infectious virus particles in the supernatants of the BLCL+DC co-culture showed efficient virus replication and stable virus titer over time (~1 logarithmic increase of $TCID_{50}$/ml) within the same period of time. Very few, if any, new infectious virus particles were produced by BLCL inoculated with t0 or t6 DC supernatants (**Fig 5D**). Together, the results suggested that imDCs are capable to transmit virus to other susceptible immune cells, such as B cells, which subsequently become productively infected.

Discussion

The systemic dissemination of EV-D68 is an essential step for extra-respiratory spread of the virus and the development of associated complications, such as AFM, but the underlying mechanism of how viruses spread to the circulation or the origin of virus in blood is largely unknown. In this study, we reveal the potential role of immune cells in the systemic dissemination of EV-D68. We show that human B cells and DCs are susceptible and permissive to EV-D68 infection and that DCs may play a role in the transmission of virus to B cells.

Immune cells are susceptible to infection of other members of *Picornaviridae*. Coxsackievirus type B infects murine splenic B cells resulting in production of new virus particles (29). Poliovirus productively infects DCs and macrophages *in vitro* (human PBMC) and *in vivo* (non-human primates) (30, 31). Echoviruses and EV-A71 have also been reported to infect human imDCs and mDCs (32, 33). Here, we showed that primary human B cells and DCs are susceptible and permissive to EV-D68 infection, which fits with findings in a cohort study that detected enterovirus RNA in peripheral blood B cells and DCs (34). In B cells, this tropism is facilitated by the presence of α2,6- and/or α2,3-linked SAs. Productive infection was only detected in BLCLs and lentivirus-transduced B cells; the latter resembles activated germinal center B cells (35). Additionally, imDCs were more susceptible and permissive to EV-D68 infection than mDCs. Therefore, it is possible that activation or maturation state of immune cells play a role in the susceptibility and permissiveness to EV-D68 infection, similar to what is observed in poliovirus (30). Furthermore, it may be that the different susceptibility to EV-D68 between imDCs and mDCs is due to higher expression of α2,6-linked SA on imDCs than mDCs (36).

We observed differences in the susceptibility and permissiveness to EV-D68 infection among viruses or donors included in this study. Differences in the susceptibility for different EV-D68 clades were observed in B cells within the PBMCs, but this was not observed in BLCLs and lentivirus-transduced B cells. Donor variation was observed in PBMCs and all B cell models and, in one PBMC donor, we observed monocytes infected with EV-D68 isolate from subclade A. The underlying mechanism for these differences among donors and possibly among different virus clades, as well as their association with the risk of the development of extra-respiratory diseases, are still unclear.

Virus replication within immune cells and/or lymphoid tissues is likely important for the development of a viremia. Due to the susceptibility and permissiveness of immune cells to EV-D68 infection, an immune cell-rich

environment, such as a lymphoid tissue, can serve as a secondary replication site for EV-D68, from where the virus can spread into the circulation. Since poliovirus viremia is essential for virus spread to the CNS and the subsequent development of CNS diseases (37), it can be speculated that EV-D68 viremia is essential for virus entry into the CNS and subsequent neurological complications, such as AFM (4, 13). In addition, a viremia could lead to virus spread to other organ system contributing to non-neurological complications associated with EV-D68 infection, including acute gastroenteritis, myocarditis and skin rash (38-40). Prevention of spread or productive infection in the lymphoid tissues may prevent systemic dissemination, as observed in poliovirus infection, in which vaccination prevents viral spread to other organs (41).

Based on our findings, we propose a model that explains the systemic dissemination of EV-D68 (**Fig 6**). EV-D68 infects respiratory epithelial cells, which results in the production of infectious virus particles and the recruitment of immune cells, such as imDCs. From the respiratory tract, cell-free virus can spill over into the circulatory and lymphatic systems and spread into lymphoid tissues. Alternatively, imDCs can become infected, and migrate to the lymphoid tissues, where they release newly produced viruses or spread virus to resident DCs or B cells. Lymphoid tissues can be the secondary replication site for EV-D68, from where the virus is released in the bloodstream. Prevention of virus spread to and amplification in lymphoid tissues can therefore prevent the development of a subsequent viremia and severe extra-respiratory complications caused by EV-D68.

Materials and methods

Ethics statement

PBMC were obtained from healthy adult donors after obtaining written informed consent. The studies were approved by the medical ethical committee of Erasmus MC, the Netherlands (MEC-2015-095). For experiment involving human buffy coats, written informed consent for research use was obtained by the Sanquin blood bank.

Cells

Human PBMC were isolated from blood (n = 8 healthy donors) by Ficoll density gradient centrifugation. BLCL were established from 5 donors by transformation with Epstein-Barr virus as previously described (42). PBMC and BLCL were cultured in RPMI-1640 medium (Capricorn) supplemented with 10% fetal bovine serum (FBS) and 100 IU/ml of penicillin, 100 µg/ml of_streptomycin and 2 mM L-glutamine (PSG). After virus inoculation, supernatants and cell lysates were collected and frozen and thawed three times prior to sample processing.

Germinal center-like primary B cell clones were generated from 3 donors. Synthetic cDNA encoding a self-cleaving polyprotein Bcl-6.t2A.Blc-xL to express the germinal center B cell-associated transcription factors Bcl-6 and Bcl-xL was synthesized (B6L; Integrated DNA Technologies) and cloned in pENTR/D-TOPO (Thermo Fisher), generating pENTR.B6L (35, 43). The B6L cDNA was subsequently transferred to pLenti6.3/V5-DEST using Gateway LR Clonase II (Thermo Fisher), generating pLV-B6L. Subsequently, lentiviral vector stocks (LV-B6L) were generated, all according to manufacturer's instructions (Thermo Fisher). Primary $CD19^+$ B-cells were isolated from human PBMC using the EasySep human CD19 positive selection kit II (StemCell Technologies) and transduced using LV.B6L as described elsewhere (35). LV-B6L transduced B cells were cultured in AIM-V AlbuMAX medium (Gibco) supplemented with 10% FBS, PSG, 50 µM beta-mercaptoethanol (Sigma), 25 ng/ml recombinant human IL-21 (Peprotech) and growth-arrested 40 gray gamma-irradiated L-CD40L feeder cells. Every 3 to 4 days, culture medium was refreshed with 25 ng/ml recombinant human IL-21 and new growth-arrested 40 gray gamma-irradiated L-CD40L feeder cells. Clonal B cell cultures from each donor were generated using limiting dilution. Absence of antibody reactivity towards EV-D68 was confirmed to exclude antibody mediated effects on EV-D68 infection (data not shown). After virus inoculation, supernatants and cell lysates were collected and frozen and thawed three times prior to sample processing.

Human rhabdomyosarcoma (RD) cells were cultured in DMEM (Lonza) supplemented with 10% FBS and PSG.

Viruses

EV-D68 strains included in this study were isolated from clinical specimens at the National Institute of Public Health and the Environment (RIVM), Bilthoven, the Netherlands. The viruses were isolated on RD cells (ATCC) at 33°C at RIVM from respiratory samples from patients with EV-D68-associated respiratory disease. Virus stocks for the studies were grown in RD cells at 33°C in 5% CO_2. The viruses included in this study with virus reference number, year of isolation an accession number are as follows: clade A (or A1) (4311200821; 2012, accession number MN954536), clade D (or A2) (4311400720; 2014, accession number MN954537) and subclade B2 (4311201039; 2012, accession number MN954539). All virus stocks were sequenced for their whole genome, and that there was no evidence for cell culture adaptive mutations.

Virus titration

Virus titers were assessed by end-point titrations in RD cells and were expressed in median tissue culture infectious dose ($TCID_{50}$/ml). In brief, 10-fold serial dilutions of a virus stock were prepared in triplicate and inoculated onto a monolayer of RD cells. The inoculated plates were incubated at 33°C in 5% CO_2. Cytopathic effect (CPE) was determined at day 5, and virus titers were determined using the Spearman-Kärber method (44).

Differentiation of monocyte-derived DCs

Human monocytes were isolated from buffy coats (n= 5 donors) by Ficoll density gradient centrifugation and selected for $CD14^+$ cells using magnetic beads. Monocytes were cultured in RPMI-1640 medium supplemented with 1XGlutamax, 10% FBS, 100 IU/ml of penicillin and 100 µg/ml of streptomycin. Subsequently, monocytes were differentiated into imDCs in the presence of human interleukin 4 (IL-4; 20ng/ml; PEPROTECH; 200-04) and human granulocyte-macrophage colony-stimulating factor (GM-CSF; 20ng/ml; MILTENYI BIOTEC; 130-093-866). At day 5, monocyte-derived imDCs were further differentiated into mature DCs by adding lipopolysaccharide (LPS; 1ug/ml; Thermo Fisher Scientific; L8274-10MG) into the medium. mDCs were defined by the increased expression of HLA-DR, CD86, PD-L1 and CD83 compared to imDCs (**S1 Fig**) and the determination of the cellular marker expression by flow cytometry is described below.

EV-D68 infection of PBMC, BLCL and lentivirus-transduced B cells

Freshly isolated PBMCs, BLCLs or lentivirus-transduced B cells (1×10^6 cells) were inoculated with EV-D68 at multiplicity of infection (MOI) of 0.1 for 1 h at 37°C in 5% CO_2. The inoculum was removed and cells were seeded in new medium into a U-bottomed 96-well plate. Cells and supernatants were collected at 0, 6, 8, 12, 24, 48 and 72 h post-inoculation (hpi). The collected specimens were frozen and thawed three times to allow release of intracellular virus before further used for virus titration. Cells were also collected at 6, 24, 48 and 72 hpi for detection of intracellular capsid protein VP1 (10 µg/ml; GeneTex; GTX132313) by flow cytometry as described below.

Removal of cell surface sialic acids on BLCL

BLCLs were incubated with 50 mU/ml *Arthrobacter ureafaciens* neuraminidase (Roche) in serum-free medium for 2 h at 37°C in 5% CO_2. Removal of α(2,3)-linked and α(2,6)-linked sialic acids on the cell surface was verified by staining with biotinylated *Maackia amurensis* lectin (MAL) I (5 µg/ml; Vector Laboratories; B-1265-1) or fluorescein-labeled *Sambucus nigra* lectin (SNA) (5 µg/ml; EY Laboratories; BA-6802-1), respectively. Biotin was detected using a streptavidin-conjugated AlexaFluor488 (5 µg/ml; Thermo Fisher Scientific; S11223). Virus and mock inoculations in non-enzymatic-treated cells were included as positive and negative infection controls, respectively. Infection of BLCL in different conditions were performed as describe above and intracellular capsid protein VP1 were detected by flow cytometry as described below.

EV-D68 inoculation of DCs and co-culture assays

ImDCs and mDCs in a flat-bottomed 96-well plate (1×10^5 cells/well) were inoculated with EV-D68/A at MOI of 1. After 1 h, the inoculum was removed and the monocytes-derived imDCs were supplemented with complete RPMI-1640 containing human IL-4 and GM-CSF, while mDCs were supplemented with complete RPMI-1640 containing human IL-4, GM-CSF and LPS. Cells and supernatants were collected at 0, 2, 4, 6, 8, 10, 24 and 48 hpi for virus titration or at 6 hpi for detection of intracellular expression of capsid protein VP1 by flow cytometry as described below.

For co-culture assay, infected imDCs (1×10^5 cells/well) as describe above were incubated with (2×10^5 BLCL/well; BLCL+DC) or without autologous BLCL (DC only). To investigate whether imDCs transfer virus particles directly to autologous BLCL or indirectly by release of infectious virus, the supernatant from imDCs that were infected

with EV-D68/A for 6 hours, were transferred to autologous BLCL (BLCL+t6 DC sup). As a control, to show that infected BLCL is not due to the leftover of virus inoculum, supernatant from the last washing step in infected imDCs were transferred to the autologous BLCL (BLCL+t0 DC sup). The schematic representation of the co-culture assay is presented in **Fig 5A**. The intracellular expression of capsid protein VP1 was detected at 6 and 24 hpi by flow cytometry as described below. Cells and supernatant were collected to detect infectious virus particles at different time points.

Flow cytometry

For determination of leukocyte phenotypes, human PBMC were incubated with monoclonal antibodies against CD19 (PE-Cy7; Beckman Coulter; IM3628), CD3 (PerCP; BD Biosciences; 345766), CD4 (V450; BD Biosciences; 560811), CD8 (AmCyan; BD Biosciences; 339188), CD14 (BV711; BD Biosciences; 740773) and CD16 (AlexaFluor647; BD Biosciences; 302020). For determination of DC phenotypes, DCs were incubated with monoclonal antibodies against HLA-DR (Pacific Blue; BioLegend; 307624), CD83(PE-Cy7; BioLegend; 305326), CD86 (AF647; BioLegend; 305416) and PD-L1 (BV785; BioLegend; 320736). For determination of cell phenotypes in DC-BLCL co-cultures, the cells were incubated with monoclonal antibodies against HLA-DR (Pacific Blue; BioLegend; 307624), CD86 (AF647; BioLegend; 305416), CD19 (PE-Cy7; Beckman Coulter; IM3628). Cells were fixed and permeabilized with BD Cytofix/Cytoperm Fixation and Permeabilization kit according to the manufacturer's instructions (BD Biosciences). The presence of intracellular capsid protein VP1 was determined by staining with polyclonal rabbit anti-EV-D68 VP1 (10 µg/ml; Genetex; GTX132313) and goat anti-rabbit IgG (FITC; BD Biosciences; 554020). Flow cytometry was performed using BD FACS Lyric (BD Biosciences, USA). Data were acquired with BD Suite software and analyzed with FlowJo software. Gating strategies to define different cell phenotypes and to define $VP1^{+}$ cells are presented in **S2 – 5 Figs**.

Statistical analyses

Statistical analyses were performed using GraphPad Prism 9.0 software (La Jolla, CA, USA). Specific tests are described in the figure legends. P values of ≤ 0.05 were considered significant. All data were expressed as standard error of mean (SEM).

Funding

This work was funded by a fellowship to DvR from the Netherlands Organization for Scientific Research (VIDI contract 91718308) and the Erasmus MC Foundation. SSNA received the Royal Thai Government Scholarship supported by the Ministry of Science and Technology of Thailand to perform her doctoral study. GPvN received financial supports from the European Union's Horizon 2020 research and innovation program under grant agreements no. 874735 (VEO) and no. 101003589 (RECoVER), and the Dutch Research Council (NWO) project no. 109986 (One Health Pact). The funders had no role in study design, data collection and analysis, decision to publish or preparation of the manuscript.

Acknowledgment

The authors would like to thank Thomas Langerak, Lisa Bauer, Feline Benavides, Lonneke Leijten, Daryl Geers Laurine Rijsbergen and Rik de Swart for technical assistance, Adam Meijer for providing the virus isolates, and Rory de Vries for helpful discussion.

Reference list

1. Greninger AL, Naccache SN, Messacar K, Clayton A, Yu G, Somasekar S, et al. A novel outbreak enterovirus D68 strain associated with acute flaccid myelitis cases in the USA (2012-14): a retrospective cohort study. Lancet Infect Dis. 2015;15(6):671-82.
2. Messacar K, Abzug MJ, Dominguez SR. The Emergence of Enterovirus-D68. Microbiol Spectr. 2016;4(3).
3. Messacar K PK, Reno S, Dominguez SR. Continued biennial circulation of enterovirus D68 in Colorado. J Clin Virol. 2019;113:24-6.
4. Messacar K, Schreiner TL, Van Haren K, Yang M, Glaser CA, Tyler KL, et al. Acute flaccid myelitis: A clinical review of US cases 2012-2015. Ann Neurol. 2016;80(3):326-38.
5. Kramer R, Sabatier M, Wirth T, Pichon M, Lina B, Schuffenecker I, et al. Molecular diversity and biennial circulation of enterovirus D68: a systematic screening study in Lyon, France, 2010 to 2016. Euro Surveill. 2018;23(37).

6. KC M, A W, HL M. Increase in Acute Respiratory Illnesses Among Children and Adolescents Associated with Rhinoviruses and Enteroviruses, Including Enterovirus D68 — United States, July–September 2022.; 2022. Contract No.: 40.
7. Benschop KS, Albert J, Anton A, Andres C, Aranzamendi M, Armannsdottir B, et al. Re-emergence of enterovirus D68 in Europe after easing the COVID-19 lockdown, September 2021. Euro Surveill. 2021;26(45).
8. Wang G, Zhuge J, Huang W, Nolan SM, Gilrane VL, Yin C, et al. Enterovirus D68 Subclade B3 Strain Circulating and Causing an Outbreak in the United States in 2016. Sci Rep. 2017;7(1):1242.
9. Yip CCY LJ, Sridhar S, Lung DC, Luk S, Chan KH et al. First Report of a Fatal Case Associated with EV-D68 Infection in Hong Kong and Emergence of an Interclade Recombinant in China Revealed by Genome Analysis. Int J Mol Sci. 2017;16(18).
10. Evans WJ, Hurst BL, Peterson CJ, Van Wettere AJ, Day CW, Smee DF, et al. Development of a respiratory disease model for enterovirus D68 in 4-week-old mice for evaluation of antiviral therapies. Antiviral Res. 2019;162:61-70.
11. Zhang C, Zhang X, Dai W, Liu Q, Xiong P, Wang S, et al. A Mouse Model of Enterovirus D68 Infection for Assessment of the Efficacy of Inactivated Vaccine. Viruses. 2018;10(2).
12. Zheng HW, Sun M, Guo L, Wang JJ, Song J, Li JQ, et al. Nasal Infection of Enterovirus D68 Leading to Lower Respiratory Tract Pathogenesis in Ferrets (Mustela putorius furo). Viruses. 2017;9(5).
13. Esposito S, Chidini G, Cinnante C, Napolitano L, Giannini A, Terranova L, et al. Acute flaccid myelitis associated with enterovirus-D68 infection in an otherwise healthy child. Virol J. 2017;14(1):4.
14. Justin D. Kreuter M, Arti Barnes M, James E. McCarthy M, Joseph D. Schwartzman M, M. Steven Oberste P, C. Harker Rhodes P, MD; , et al. A fatal CNS EV68 infection. Arch Pathol Lab Med2011.
15. Kusabe Y, Takeshima A, Seino A, Nishida M, Takahashi M, Yamada S, et al. [An Adult Case of Enterovirus D68 Encephalomyelitis Presenting as Bilateral Facial Nerve Palsy and Dysphagia]. Brain Nerve. 2017;69(8):957-61.
16. Chong PF, Kira R, Mori H, Okumura A, Torisu H, Yasumoto S, et al. Clinical Features of Acute Flaccid Myelitis Temporally Associated With an Enterovirus D68 Outbreak: Results of a Nationwide Survey of Acute Flaccid Paralysis in Japan, August-December 2015. Clin Infect Dis. 2018;66(5):653-64.

17. Imamura T, Suzuki A, Lupisan S, Kamigaki T, Okamoto M, Roy CN, et al. Detection of enterovirus 68 in serum from pediatric patients with pneumonia and their clinical outcomes. Influenza Other Respir Viruses. 2014;8(1):21-4.
18. Racaniello VR. One hundred years of poliovirus pathogenesis. Virology. 2006;344(1):9-16.
19. Solomon T, Lewthwaite P, Perera D, Cardosa MJ, McMinn P, Ooi MH. Virology, epidemiology, pathogenesis, and control of enterovirus 71. Lancet Infect Dis. 2010;10(11):778-90.
20. Zhao T, Zhang Z, Zhang Y, Feng M, Fan S, Wang L, et al. Dynamic Interaction of Enterovirus 71 and Dendritic Cells in Infected Neonatal Rhesus Macaques. Front Cell Infect Microbiol. 2017;7:171.
21. Xing J, Wang K, Wang G, Li N, Zhang Y. Recent advances in enterovirus A71 pathogenesis: a focus on fatal human enterovirus A71 infection. Arch Virol. 2022.
22. He Y, Ong KC, Gao Z, Zhao X, Anderson VM, McNutt MA, et al. Tonsillar crypt epithelium is an important extra-central nervous system site for viral replication in EV71 encephalomyelitis. Am J Pathol. 2014;184(3):714-20.
23. Smura T, Ylipaasto P, Klemola P, Kaijalainen S, Kyllonen L, Sordi V, et al. Cellular tropism of human enterovirus D species serotypes EV-94, EV-70, and EV-68 in vitro: implications for pathogenesis. J Med Virol. 2010;82(11):1940-9.
24. Laksono BM, Grosserichter-Wagener C, de Vries RD, Langeveld SAG, Brem MD, van Dongen JJM, et al. In Vitro Measles Virus Infection of Human Lymphocyte Subsets Demonstrates High Susceptibility and Permissiveness of both Naive and Memory B Cells. J Virol. 2018;92(8).
25. Sakabe S, Iwatsuki-Horimoto K, Takano R, Nidom CA, Le MTQ, Nagamura-Inoue T, et al. Cytokine production by primary human macrophages infected with highly pathogenic H5N1 or pandemic H1N1 2009 influenza viruses. J Gen Virol. 2011;92(Pt 6):1428-34.
26. Videira PA, Amado IF, Crespo HJ, Algueró MC, Dall'Olio F, Cabral MG, et al. Surface alpha 2-3- and alpha 2-6-sialylation of human monocytes and derived dendritic cells and its influence on endocytosis. Glycoconj J. 2008;25(3):259-68.
27. Eash S, Tavares R, Stopa EG, Robbins SH, Brossay L, Atwood WJ. Differential distribution of the JC virus receptor-type sialic acid in normal human tissues. Am J Pathol. 2004;164(2):419-28.
28. Cao W, Liu YJ. Innate immune functions of plasmacytoid dendritic cells. Curr Opin Immunol. 2007;19(1):24-30.

29. Mena I, Perry CM, Harkins S, Rodriguez F, Gebhard J, Whitton JL. The role of B lymphocytes in coxsackievirus B3 infection. Am J Pathol. 1999;155(4):1205-15.
30. Wahid R, Cannon MJ, Chow M. Dendritic Cells and Macrophages Are Productively Infected by Poliovirus. Journal of Virology. 2005;79(1):401-9.
31. Shen L, Chen CY, Huang D, Wang R, Zhang M, Qian L, et al. Pathogenic Events in a Nonhuman Primate Model of Oral Poliovirus Infection Leading to Paralytic Poliomyelitis. J Virol. 2017;91(14).
32. Kramer M, Schulte BM, Toonen LW, de Bruijni MA, Galama JM, Adema GJ, et al. Echovirus infection causes rapid loss-of-function and cell death in human dendritic cells. Cell Microbiol. 2007;9(6):1507-18.
33. Lin YW, Wang SW, Tung YY, Chen SH. Enterovirus 71 infection of human dendritic cells. Exp Biol Med (Maywood). 2009;234(10):1166-73.
34. Sioofy-Khojine AB, Richardson SJ, Locke JM, Oikarinen S, Nurminen N, Laine AP, et al. Detection of enterovirus RNA in peripheral blood mononuclear cells correlates with the presence of the predisposing allele of the type 1 diabetes risk gene IFIH1 and with disease stage. Diabetologia. 2022.
35. Kwakkenbos MJ, Diehl SA, Yasuda E, Bakker AQ, van Geelen CM, Lukens MV, et al. Generation of stable monoclonal antibody-producing B cell receptor-positive human memory B cells by genetic programming. Nat Med. 2010;16(1):123-8.
36. Jenner J, Kerst G, Handgretinger R, Muller I. Increased alpha2,6-sialylation of surface proteins on tolerogenic, immature dendritic cells and regulatory T cells. Exp Hematol. 2006;34(9):1212-8.
37. Horstmann DM. Poliomyelitis virus in blood of orally infected monkeys and chimpanzees. Proc Soc Exp Biol Med. 1952;79(3):417-9.
38. Pham NTK, Thongprachum A, Baba T, Okitsu S, Trinh QD, Komine-Aizawa S, et al. A 3-Month-Old Child with Acute Gastroenteritis with Enterovirus D68 Detected from Stool Specimen. Clin Lab. 2017;63(7):1269-72.
39. Antona D, Kossorotoff M, Schuffenecker I, Mirand A, Leruez-Ville M, Bassi C, et al. Severe paediatric conditions linked with EV-A71 and EV-D68, France, May to October 2016. Eurosurveillance. 2016;21(46):11-4.
40. Chang TH, Yang TI, Hsu WY, Huang LM, Chang LY, Lu CY. Case report: painful exanthems caused by enterovirus D68 in an adolescent. Medicine (Baltimore). 2019;98(33):e16493.
41. Zhu Q, Berzofsky JA. Oral vaccines: directed safe passage to the front line of defense. Gut Microbes. 2013;4(3):246-52.

418 42. van Binnendijk RS, Poelen MC, de Vries P, Voorma HO, Osterhaus AD, Uytdehaag FG. Measles virus-specific
419 human T cell clones. Characterization of specificity and function of CD4+ helper/cytotoxic and CD8+ cytotoxic
420 T cell clones. J Immunol. 1989;142(8):2847-54.
421 43. Wang Y, Wang F, Wang R, Zhao P, Xia Q. 2A self-cleaving peptide-based multi-gene expression system in the
422 silkworm Bombyx mori. Sci Rep. 2015;5:16273.
423 44. Atkinson GF. The Spearman-Karber Method of Estimating 50% Endpoints. Cornell University. Dept. of
424 Biometrics.: Biometrics Unit Technical Reports;; 1961. Contract No.: BU-141-M.

425

426

427 **Figures and Tables**

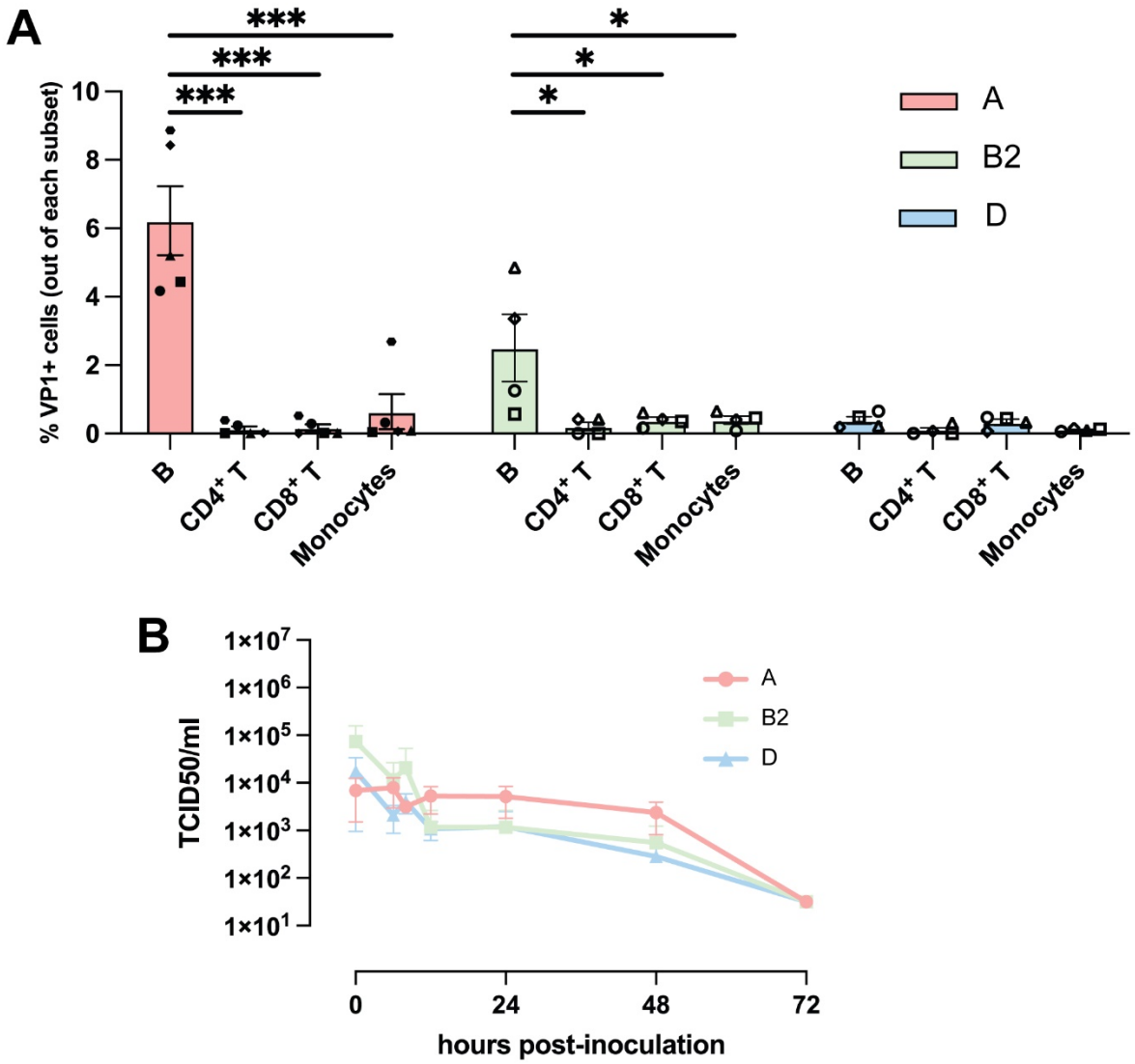

428

429 **Fig 1. Susceptibility and permissiveness of human PBMC to EV-D68 infection.** (A) Percentage of EV-D68 VP1$^+$

430 leukocyte subsets 24 h after inoculation with EV-D68 strains from subclades A (n = 5 donors), B2 (n = 4 donors)

431 and D (n = 4 donors). Each symbol represents one donor. Statistical analysis was performed using a one-way

432 ANOVA with multiple comparison test. Error bars denoted SEM. (B) Production of infectious viruses in EV-D68-

433 inoculated PBMC. PBMC: peripheral blood mononuclear cells; SEM: standard error of mean *: P<0.05; ***:

434 P≤0.001.

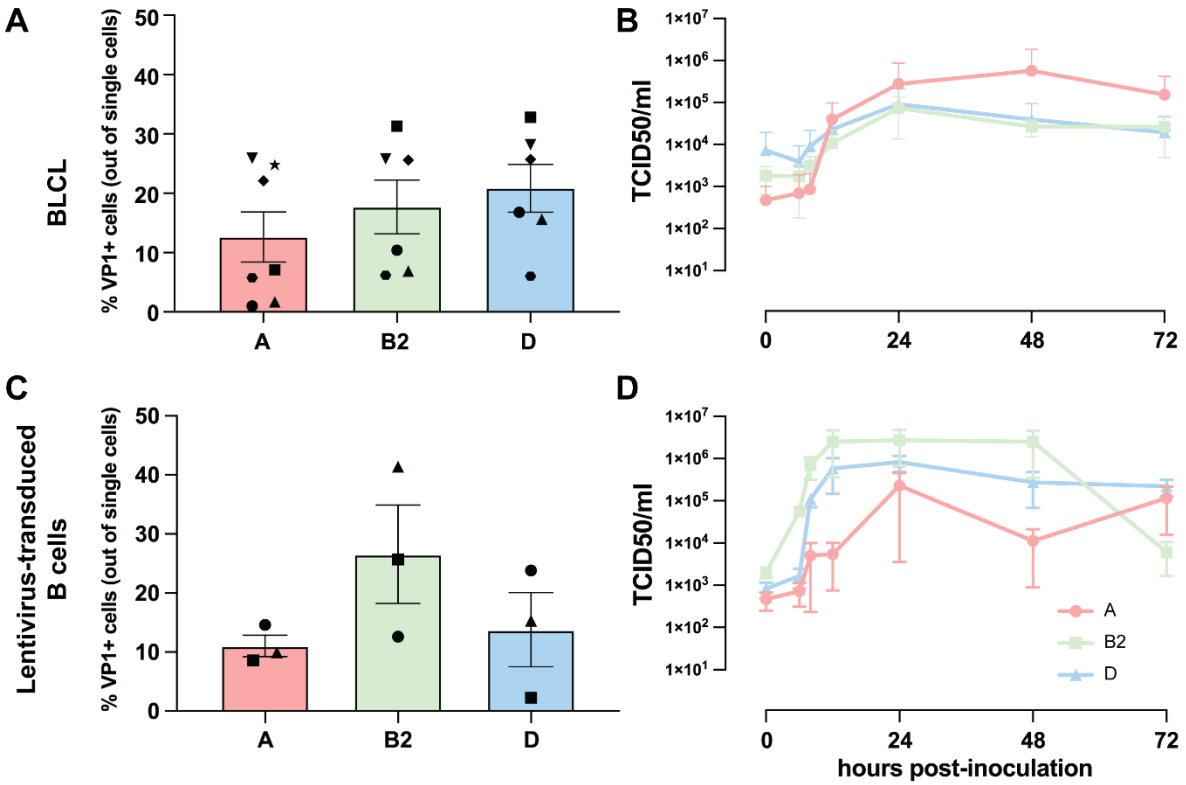

435

436 **Fig 2. Susceptibility and permissiveness of B cell-rich models to EV-D68 infection.** BLCL and lentivirus-
437 transduced B cells were inoculated with EV-D68 strains from subclades A (n = 7), B2 (n = 6) and D (n = 6) as
438 models for EV-D68 infection in B cell-rich environment. (A – B) Percentage of EV-D68 VP1⁺ cells at 24 hpi and
439 production of new infectious virus particles in EV-D68-inoculated BLCL over time, respectively. (C – D)
440 Percentage of VP1⁺ cells at 24 hpi and production of infectious viruses in EV-D68-inoculated lentivirus-
441 transduced B-cells. Each symbol in (A) and (C) represents one donor. No statistically significant differences were
442 observed in the percentages of VP1⁺ cells among the different virus clades. Statistical analysis was performed
443 using a one-way ANOVA with multiple comparison test. Error bars denote SEM. BLCL: B-lymphoblastoid cell line;
444 hpi: hours post-inoculation; SEM: standard error of mean.

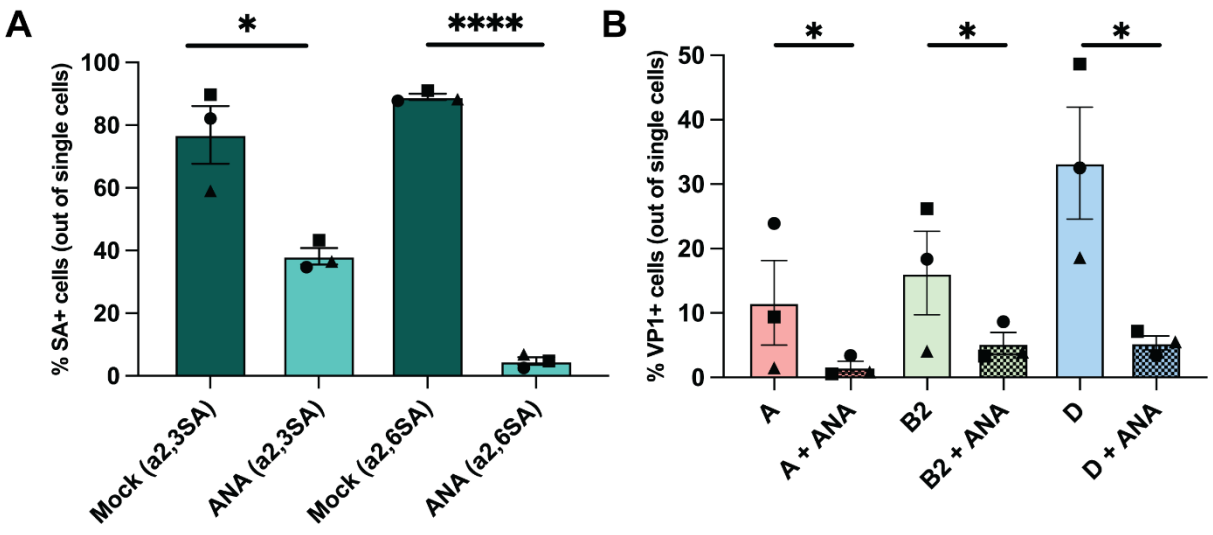

Fig 3. Percentages of α2,3-and α2,6-linked SAs⁺ and EV-D68 VP1⁺ BLCL upon neuraminidase treatment. (A) Percentage of BLCL expressed α2,3- (n=3) and α2,6- (n=3) linked SAs with and without ANA treatment. (B) Percentage of VP1⁺ BLCL (n=3) with and without ANA treatment inoculated with EV-D68 from subclades A, B2 and D, measured 24 hpi. Statistical analysis was performed with t-test. Error bars denote SEM. BLCL: B-lymphoblastoid cell line. ANA: *Arthrobacter ureafaciens* neuraminidase; SAs: sialic acids; hpi: hours post-inoculation; SEM: standard error of mean. *: P<0.05; ****: P≤0.0001.

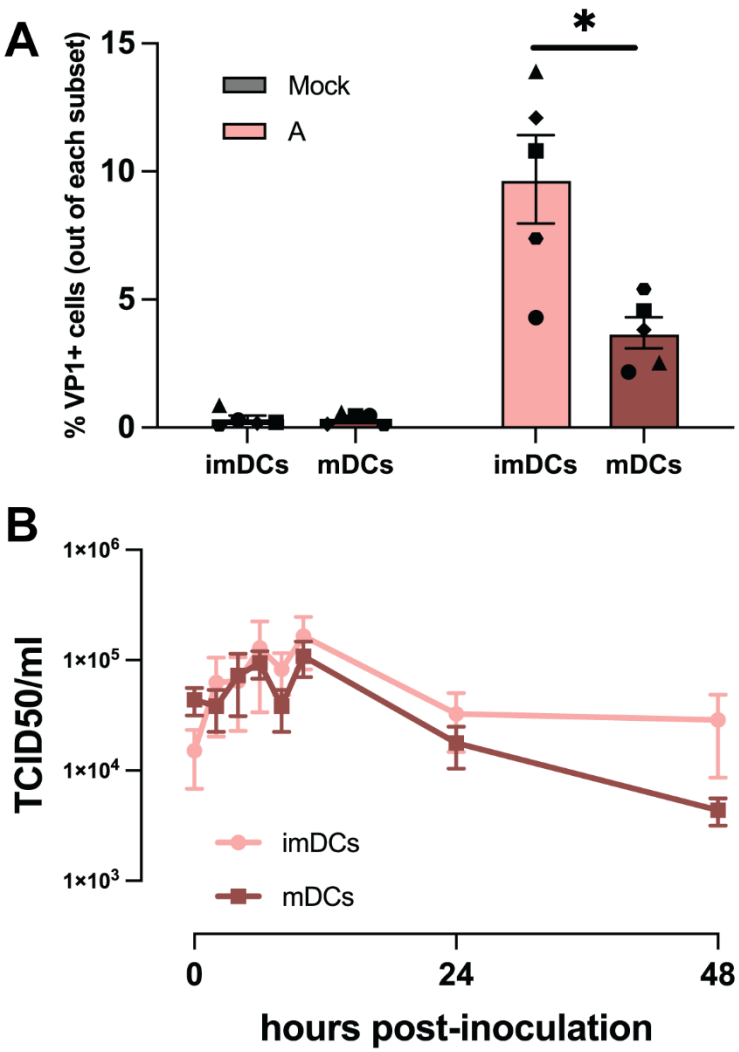

453

454 **Fig 4. Susceptibility and permissiveness of imDCs and mDCs to EV-D68 infection.** (A) Percentage of EV-D68 VP1$^+$
455 imDCs (n = 5) and mDCs (n = 5) measured at 6 hpi. (B) Production of infectious viruses in EV-D68/A-inoculated
456 imDCs (n = 3) and mDCs (n = 3). Samples for virus titration were collected at 0, 2, 4, 6, 8, 10, 24 and 48 hpi. All
457 statistical analyses in this figure were performed with t-test. Error bars denote SEM. imDCs: immature dendritic
458 cells; mDCs: mature dendritic cells; hpi: hours post-inoculation; SEM: standard error of mean. *: P<0.05; **:
459 P<0.01.

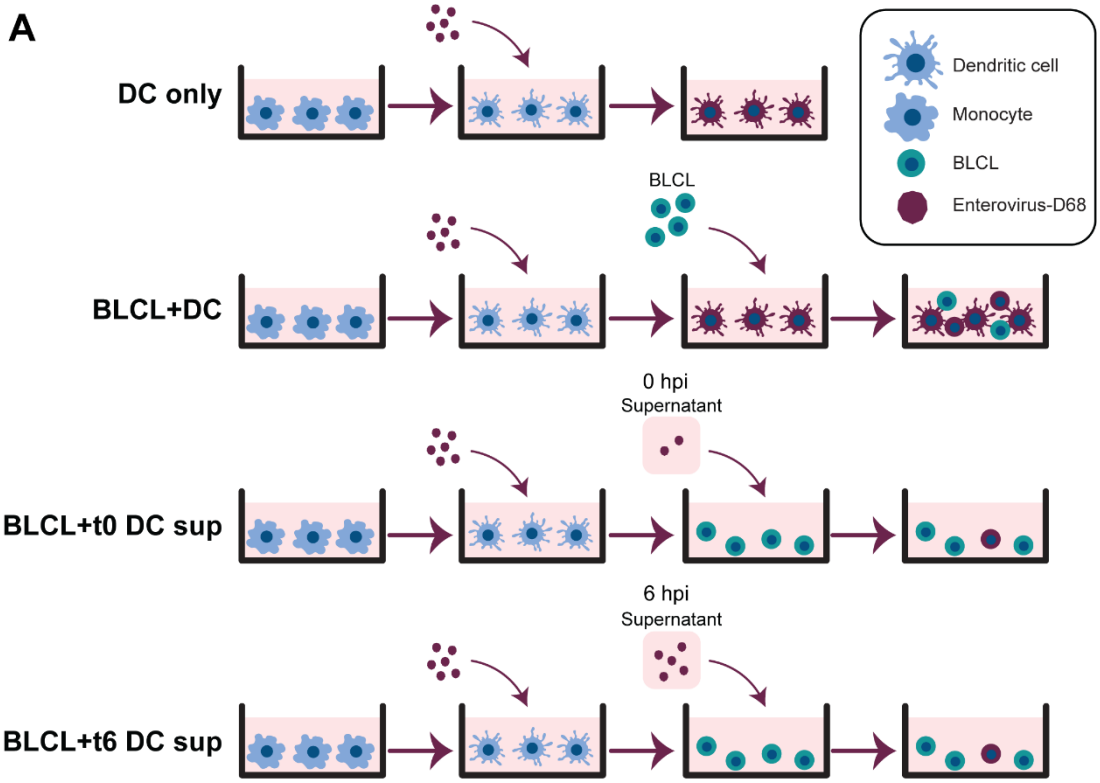

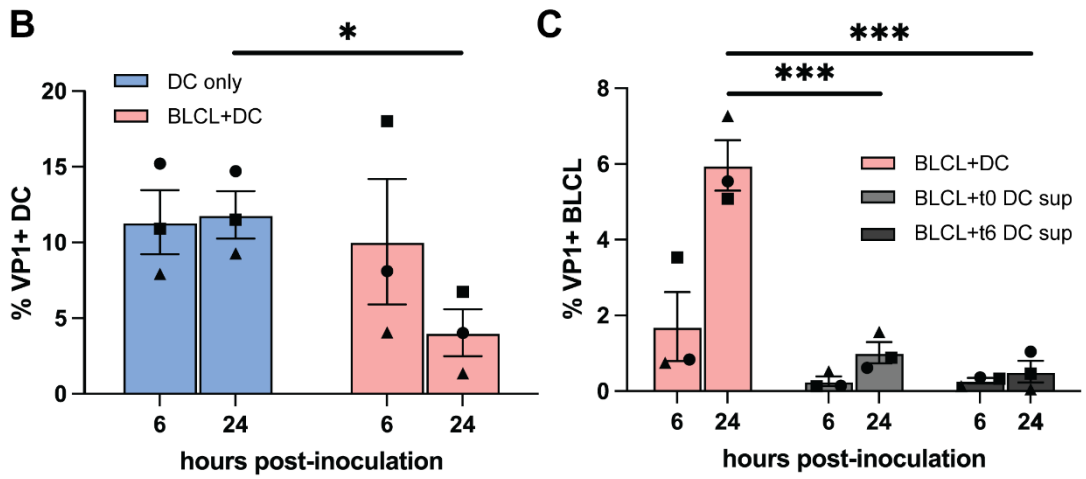

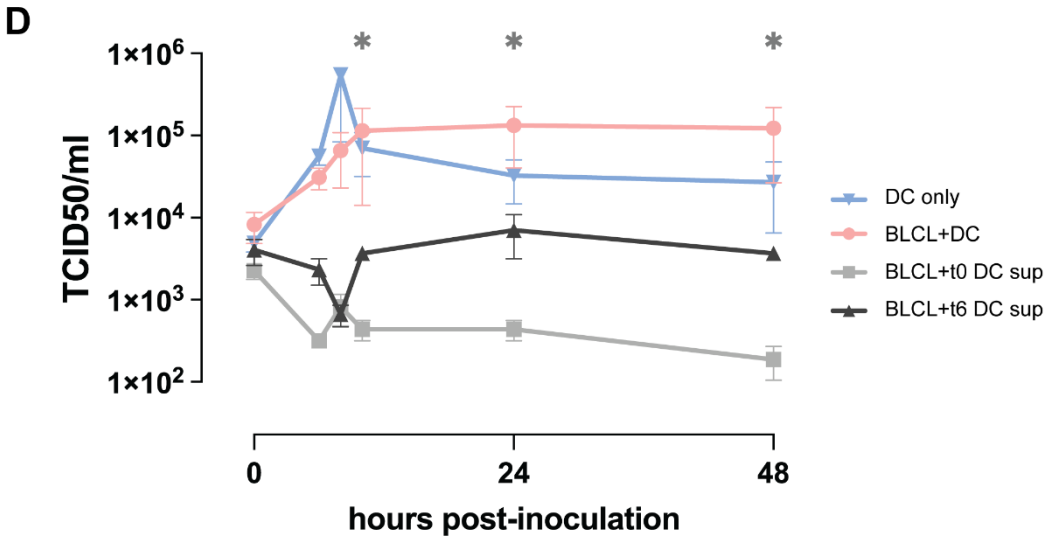

460

Fig 5. Co-culture of EV-D68-inoculated imDCs with their autologous BLCL. (A) Schematic representation of the experimental setup and controls. (B) Percentages of EV-D68 $VP1^{+}$ imDCs and (C) BLCL in different culture conditions at 6 and 24 hpi. (D) Production infectious viruses in different culture conditions. Statistical analysis in (B) was performed with t-test. Statistical analysis in (C) and (D) were performed with a one-way ANOVA with multiple comparison test and compared to BLCL+t0 DC sup and BLCL+t6 sup, respectively. Error bars denote SEM. BLCL: B-lymphoblastoid cell line; imDCs: immature dendritic cells; hpi: hours post-inoculation; SEM: standard error of mean; BLCL+t0 DC sup: autologous BLCL co-cultured with supernatant collected from EV-D68/A-inoculated imDCs at 0 hpi. BLCL+t6 DC sup: autologous BLCL co-cultured with supernatant collected from EV-D68/A-inoculated imDCs at 6 hpi. *: $P<0.05$; ***: $P\leq0.001$.

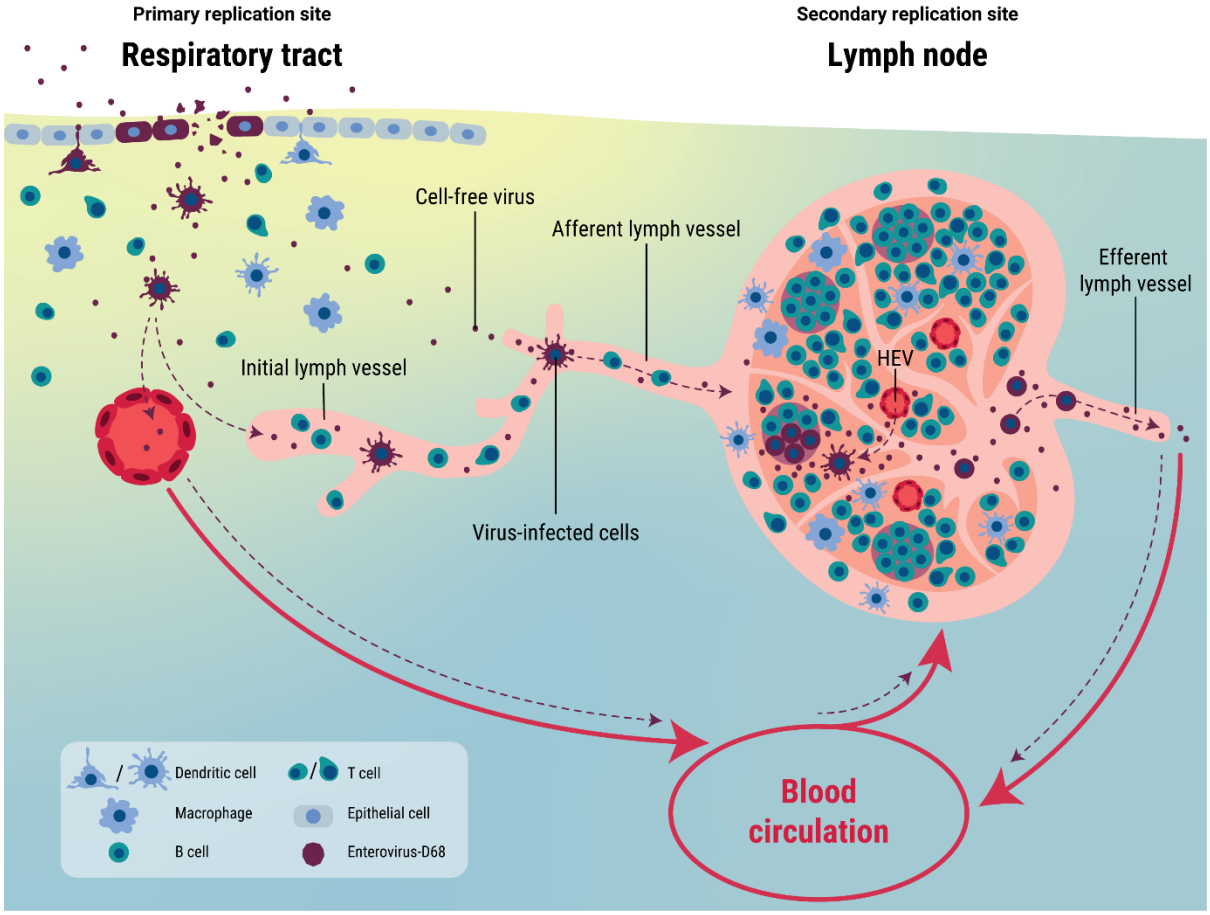

Fig 6. Proposed model for systemic dissemination of EV-D68. EV-D68 enters the respiratory tract and initially infects respiratory epithelial cells. The infection will result in the recruitment of immune cells, including imDCs. Subsequently, cell-free EV-D68 can spread to lymphoid tissues by spilling over into the circulatory or lymphatic system. Alternatively, it can infect imDCs, which can transfer the virus to lymphoid tissues. These lymphoid tissues can function as a secondary replication site, where EV-D68 infects mDCs and B cells. From this site, cell-free virus or virus-infected immune cells can enter the blood circulation and spread virus to other tissues. HEV: high endothelial venule. Red arrow: blood circulation; purple dotted arrow: potential routes of EV-D68 spread.

480 **Supplementary Information**

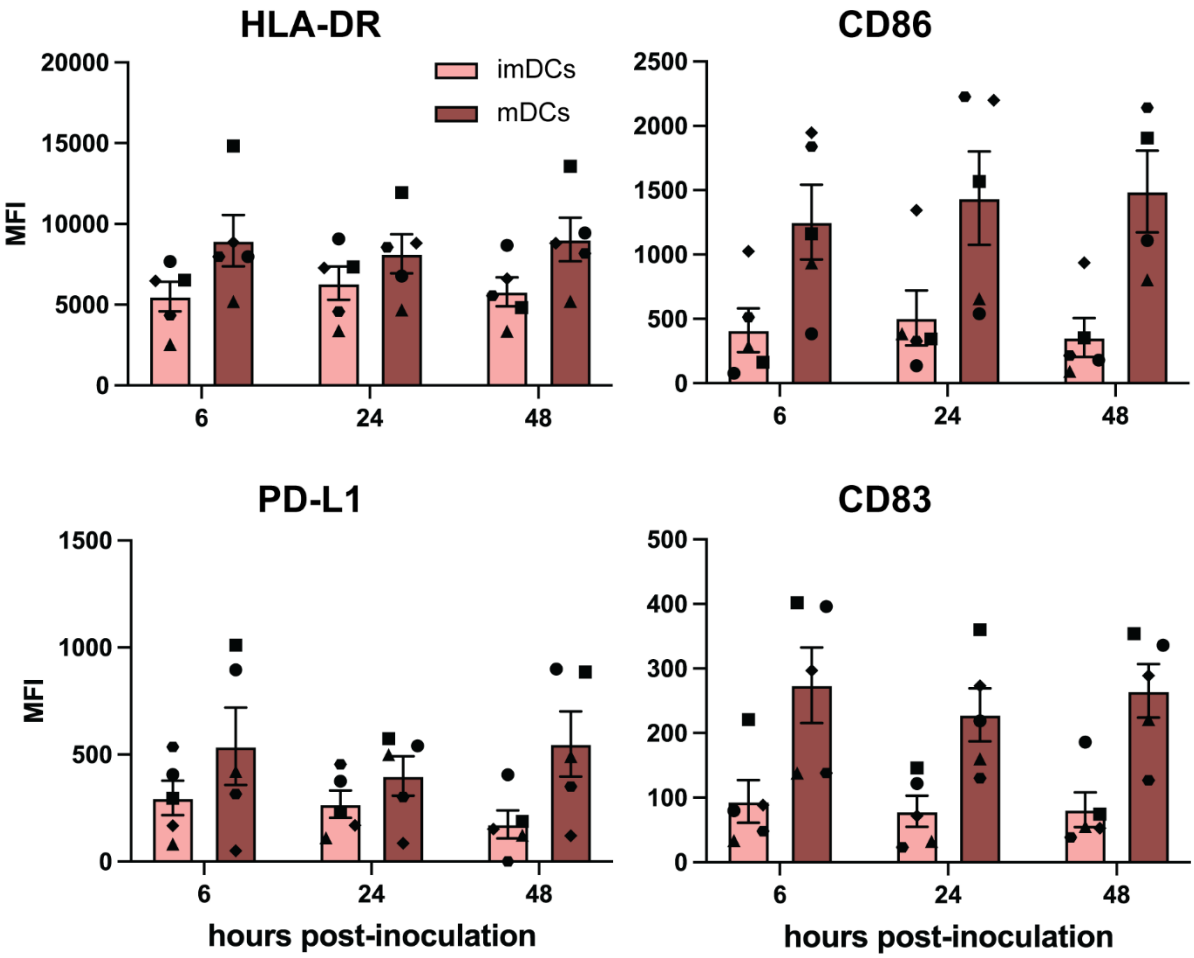

481

482 **S1 Fig. The expression of dendritic cell maturation markers in immature and mature dendritic cells (imDCs and**
483 **mDCs).** mDCs were defined by the upregulation of surface HLA-DR, CD86, PD-L1 and CD83 after treatment of
484 monocyte-derived imDCs with lipopolysacharride. Each symbol represents one donor. Error bars denote
485 standard error of mean. MFI: median fluorescence intensity.

486

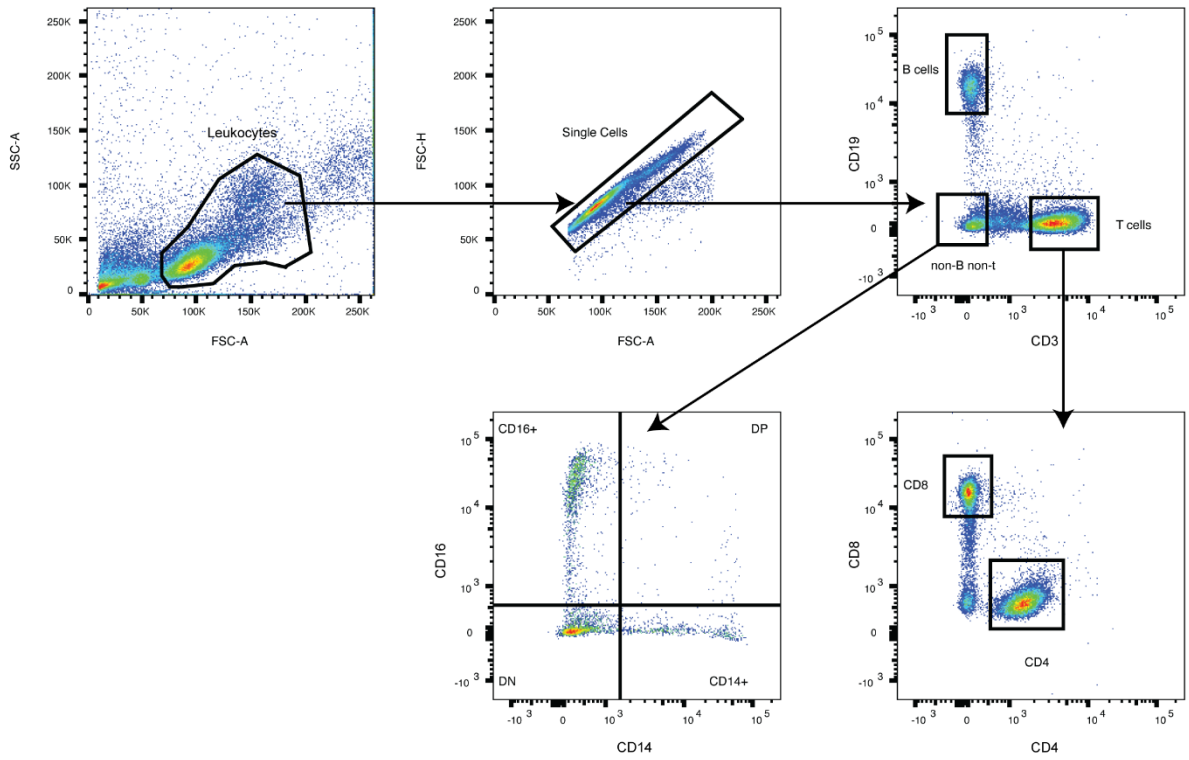

487

488 **S2 Fig. Representative gating strategy for peripheral blood mononuclear cell subpopulations.** B cells were

489 defined as $CD3^{-}CD19^{+}$ cells; $CD4^{+}$T cells as $CD3^{+}CD19^{-}CD4^{+}CD8^{-}$ cells; $CD8^{+}$T cells as $CD3^{+}CD19^{-}CD4^{-}CD8^{+}$ cells; and

490 monocytes as $CD3^{-}CD19^{-}CD14^{-/+}CD16^{-/+}$ cells.

491

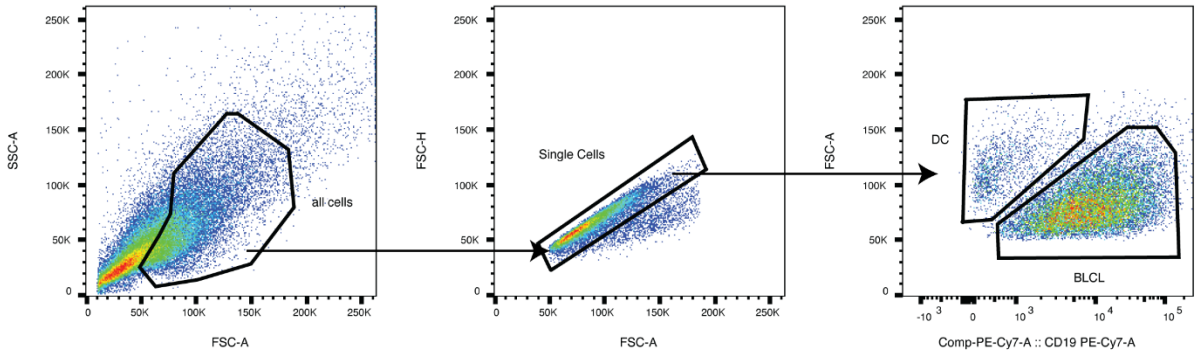

492

493 **S3 Fig. Representative gating strategy for EV-D68-inoculated immature dendritic cells (imDCs) co-cultured**

494 **with autologous B-lymphoblastoid cell line (BLCL).** imDCs were defined as $CD19^-$ cells; BLCL were defined as

495 $CD19^+$ cells.

496

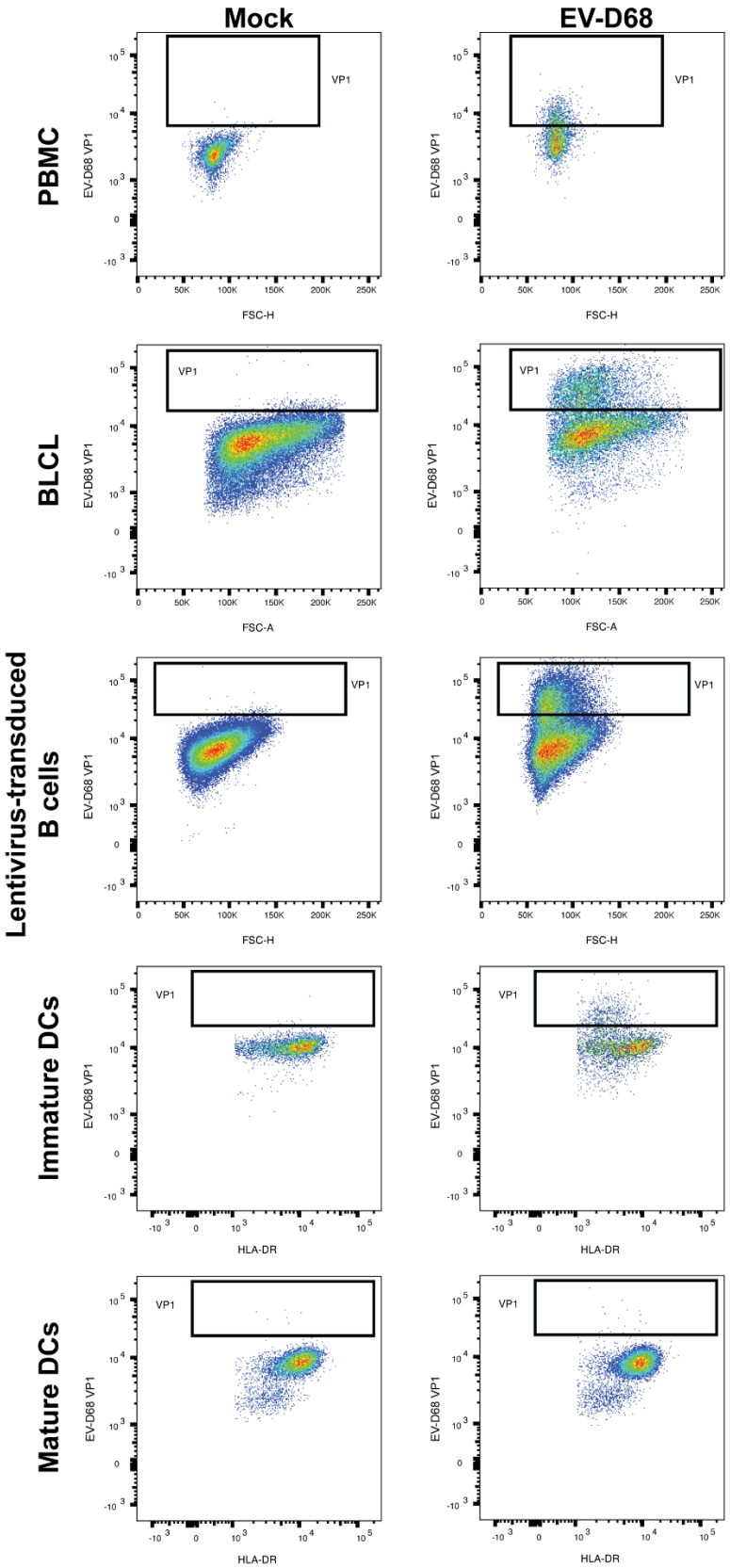

497

498 **S4 Fig. Representative gating strategies for EV-D68 VP1⁺ cells.** PBMC: peripheral blood mononuclear cells; BLCL:

499 B-lymphoblastoid cell line; DCs: dendritic cells.

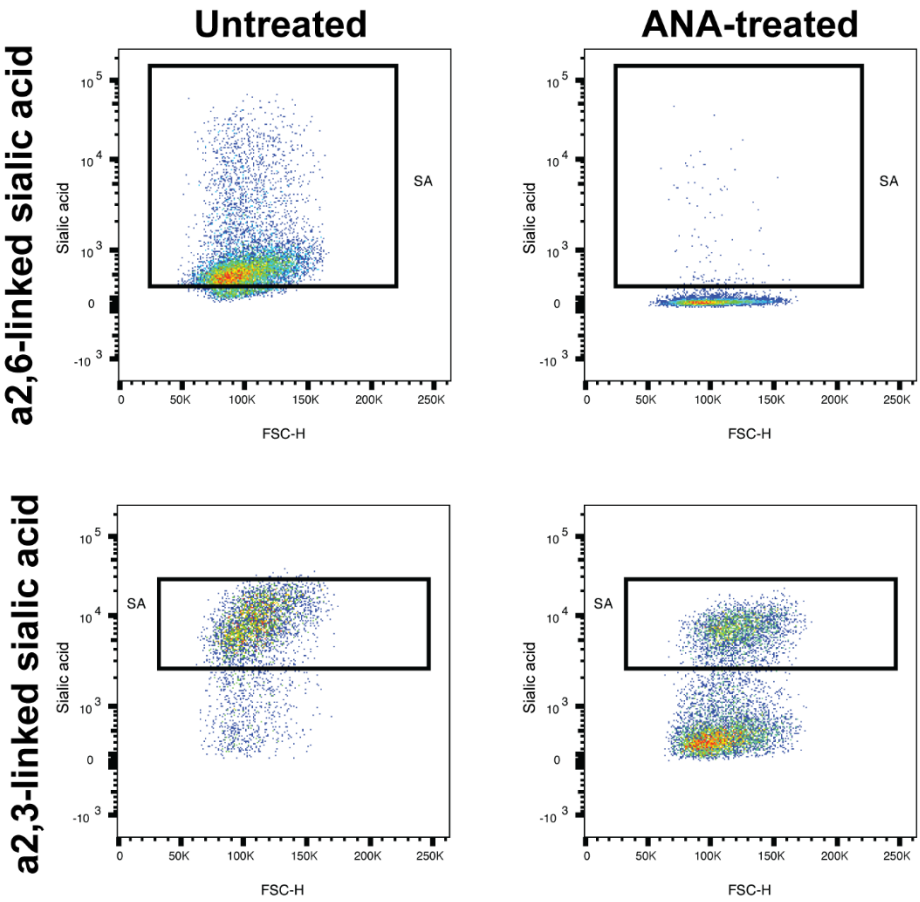

500

501 **S5 Fig. Representative gating strategy to determine percentages of α2,3- and α2,6-linked sialic acid⁺ (SAs⁺)**

502 **BLCL.** Percentages of SA⁺ cells were determined at 0 h post-inoculation. ANA: *Arthrobacter ureafaciens*

503 neuraminidase; BLCL: B-lymphoblastoid cell line.

504

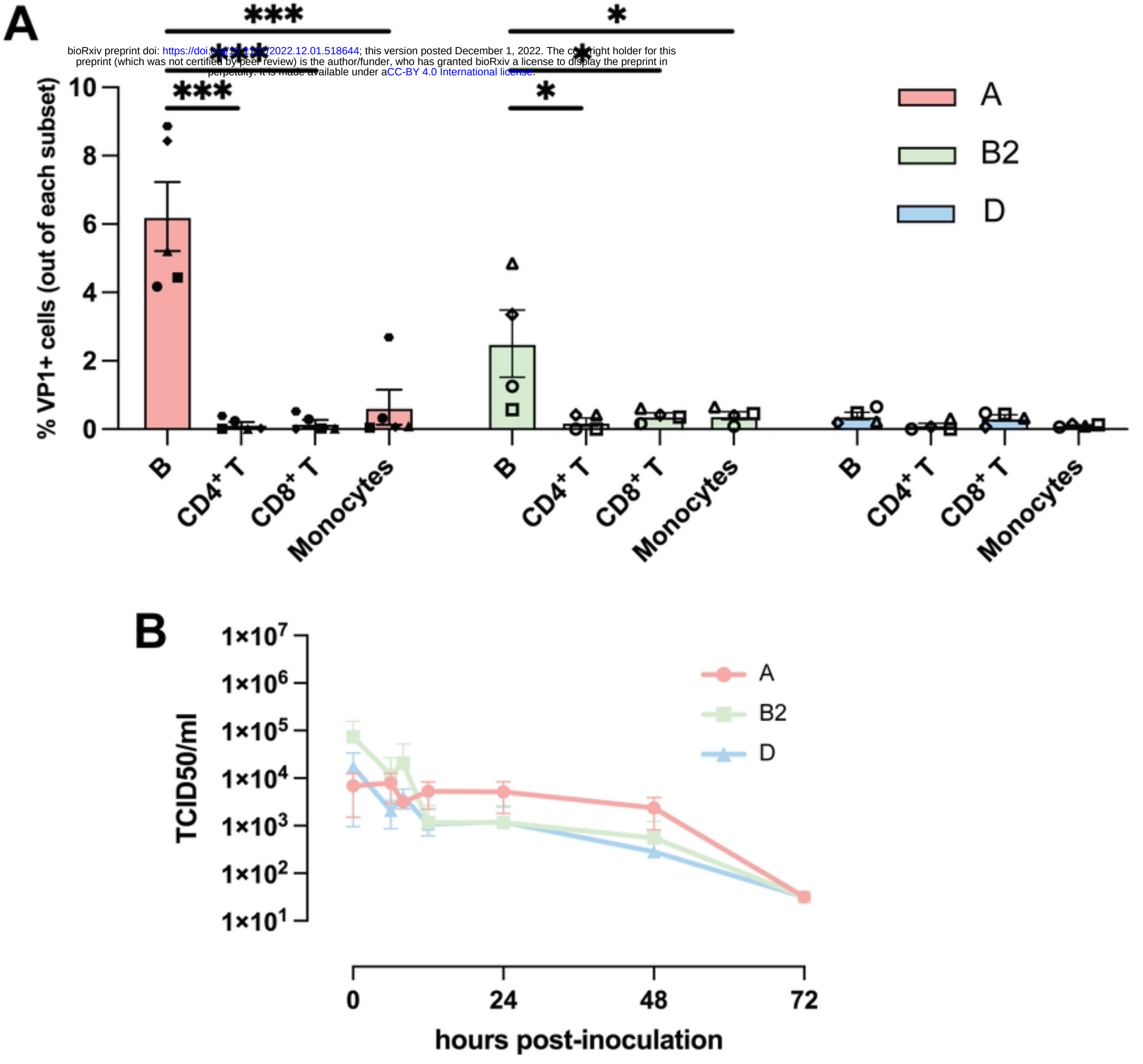

Fig 1

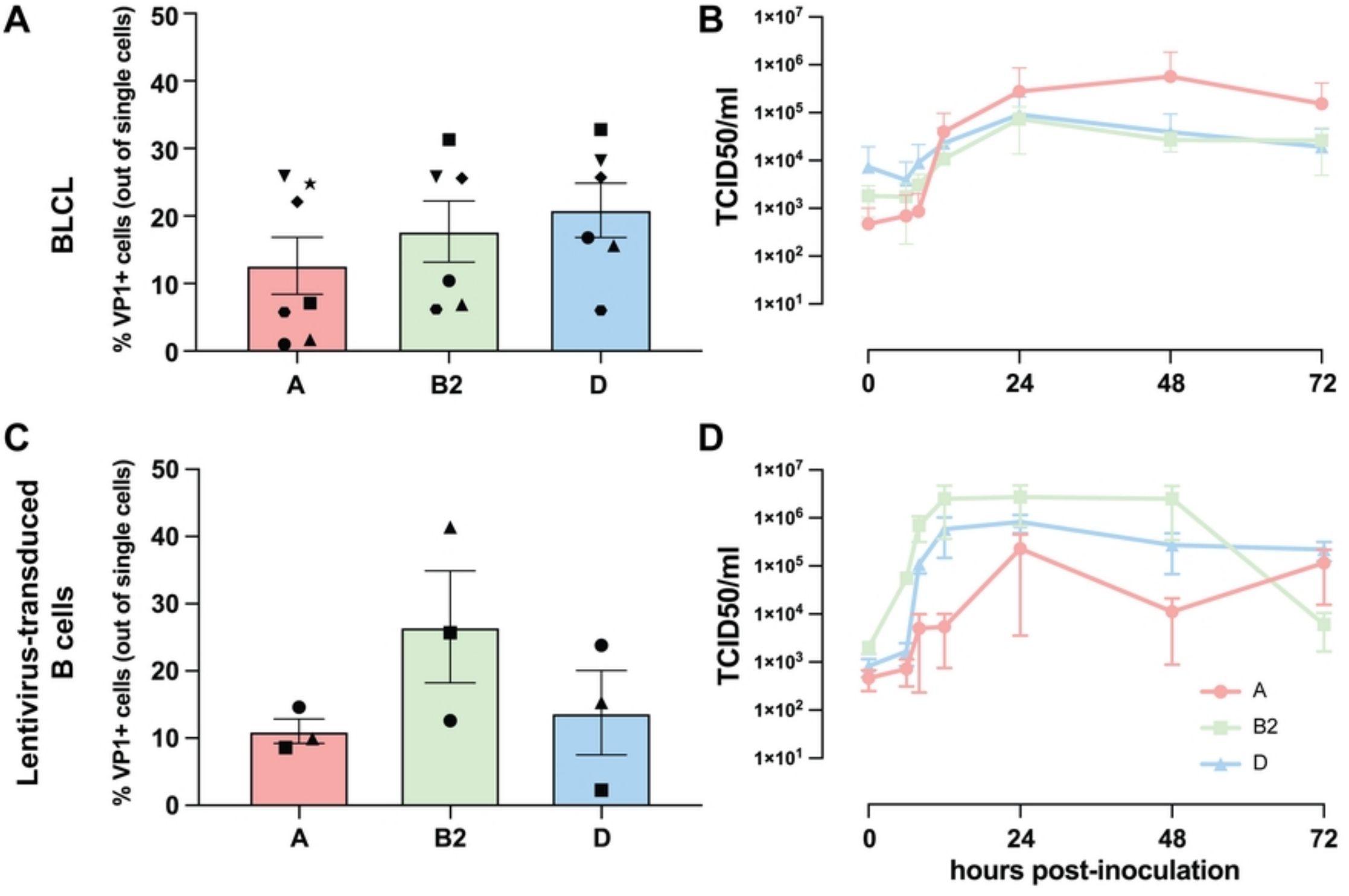
A
BLCL
% VP1+ cells (out of single cells)
50
40
30
20
10
0
A
B2
D
B
TCID50/ml
1×10⁷
1×10⁶
1×10⁵
1×10⁴
1×10³
1×10²
1×10¹
0
24
48
72
C
Lentivirus-transduced B cells
% VP1+ cells (out of single cells)
50
40
30
20
10
0
A
B2
D
D
TCID50/ml
1×10⁷
1×10⁶
1×10⁵
1×10⁴
1×10³
1×10²
1×10¹
A
B2
D
0
24
48
72
hours post-inoculation

Fig 2

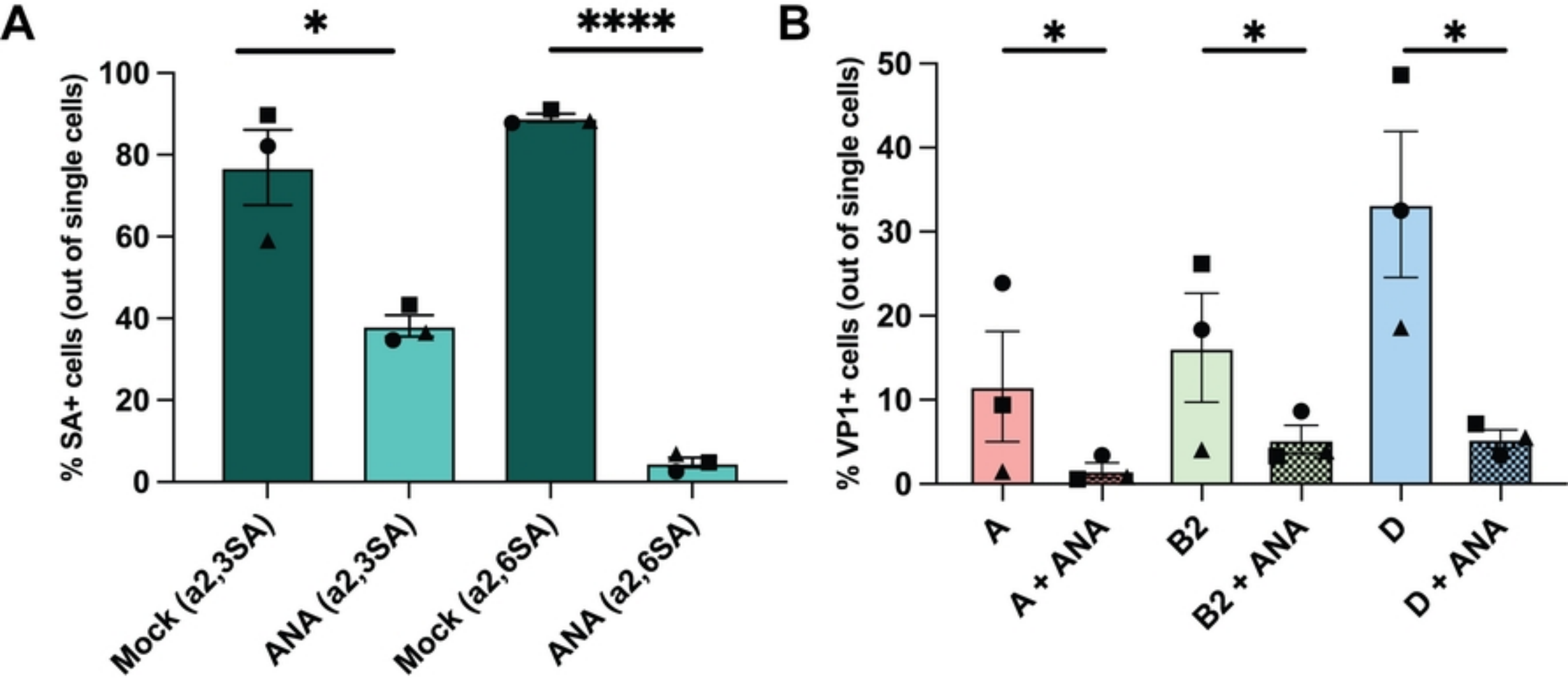
A
*
****
% SA+ cells (out of single cells)
100
80
60
40
20
0
Mock (a2,3SA)
ANA (a2,3SA)
Mock (a2,6SA)
ANA (a2,6SA)
B
*
*
*
% VP1+ cells (out of single cells)
50
40
30
20
10
0
A
A + ANA
B2
B2 + ANA
D
D + ANA

Fig 3

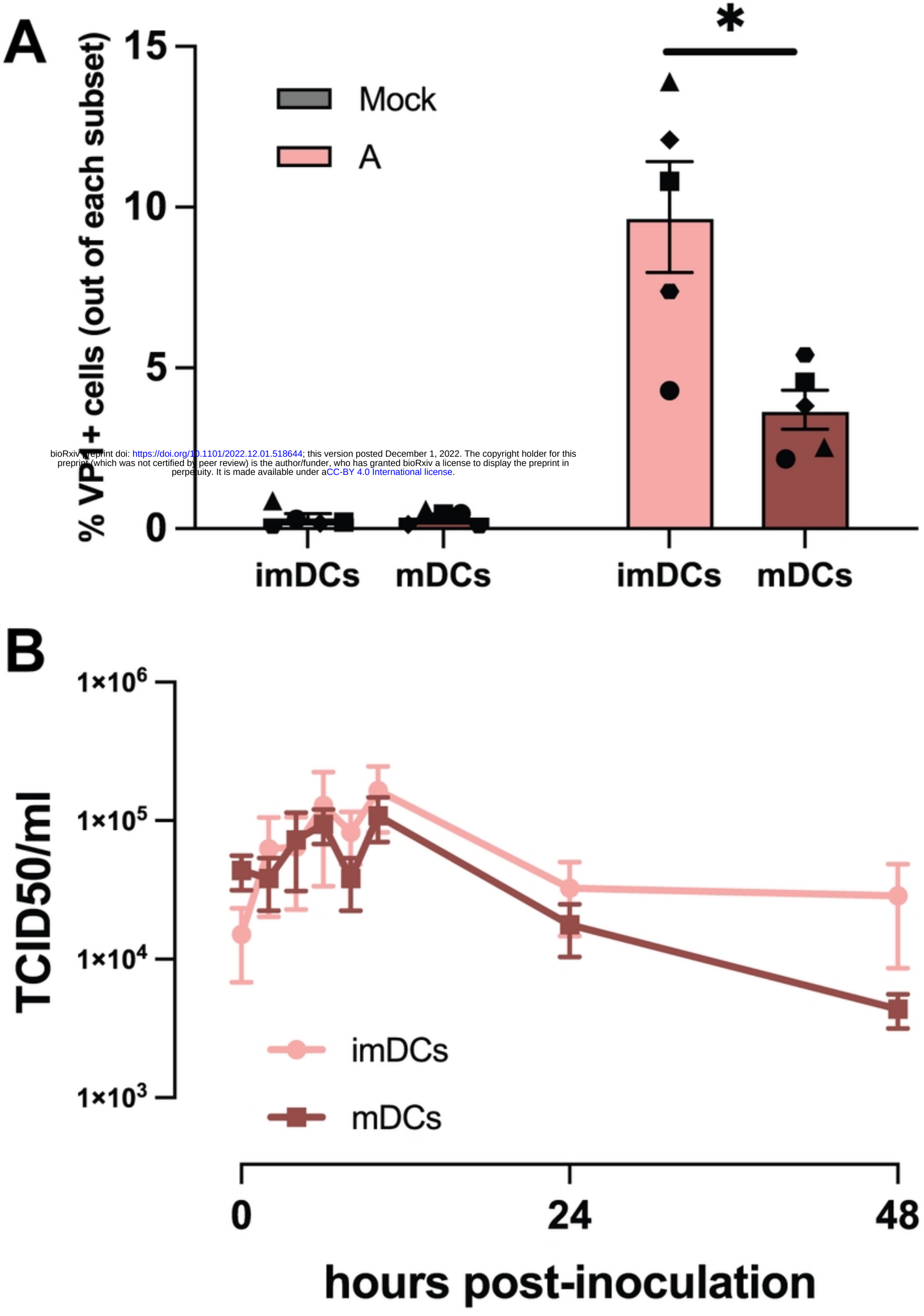

Fig 4

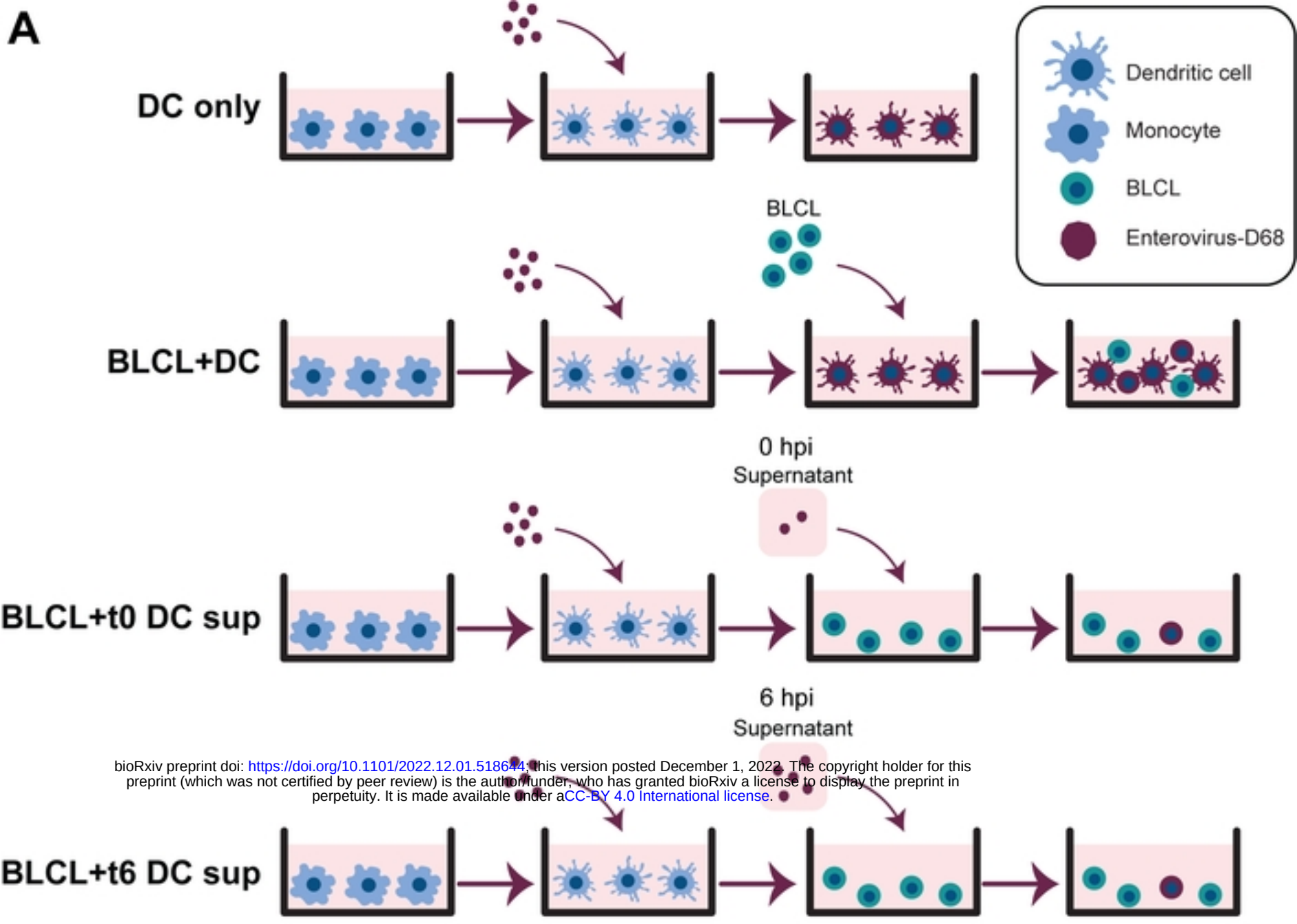

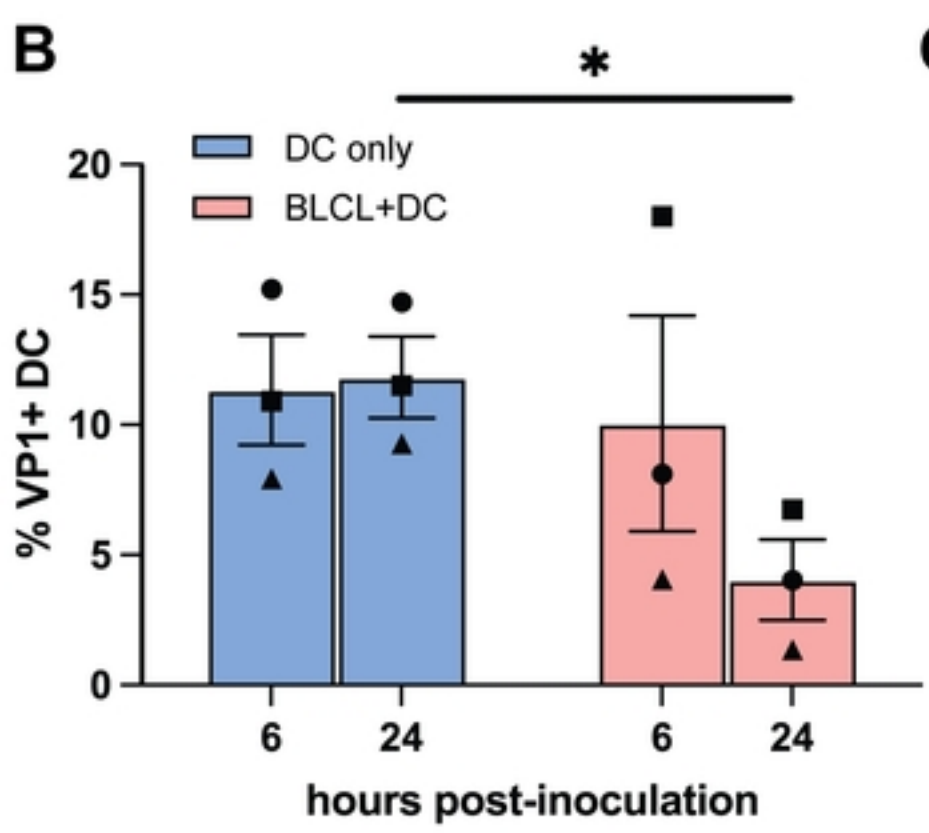

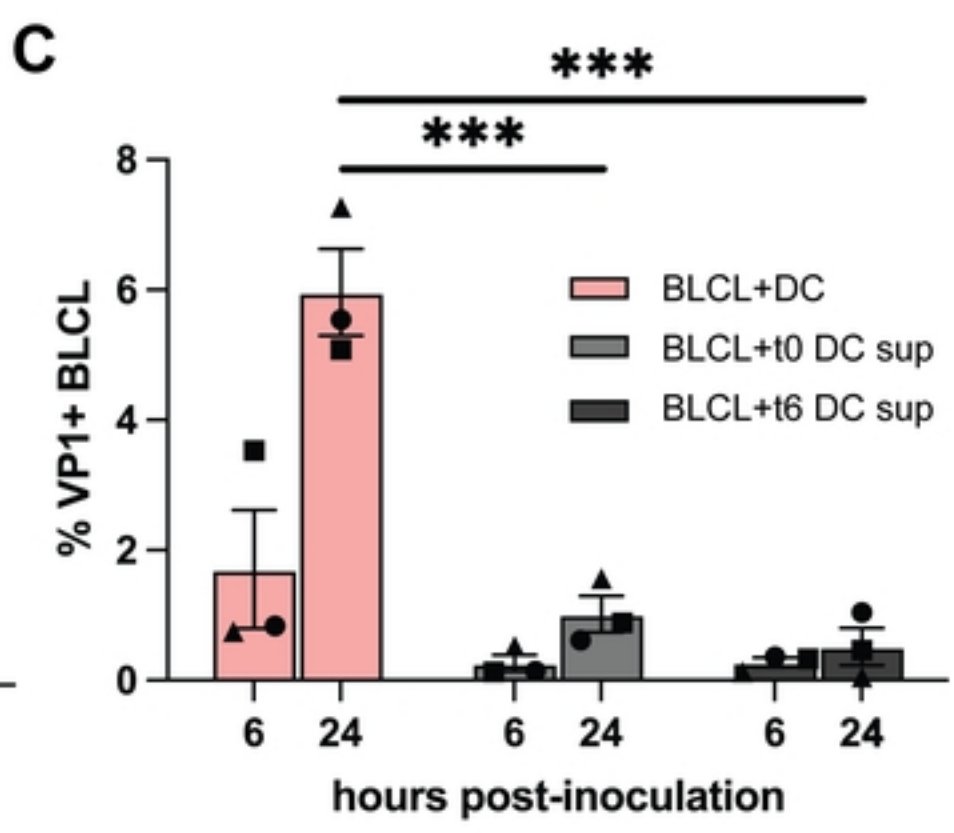

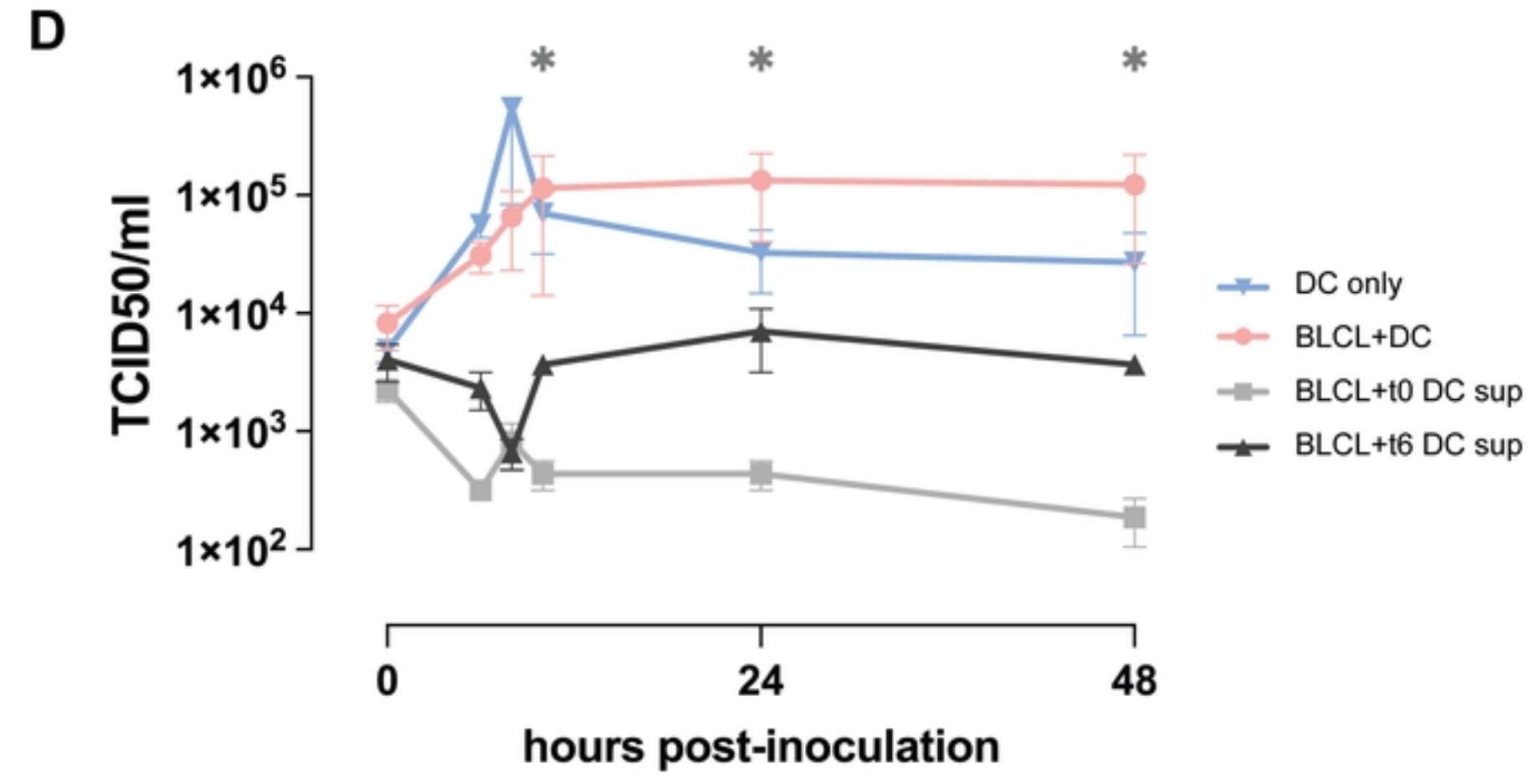

Fig 5

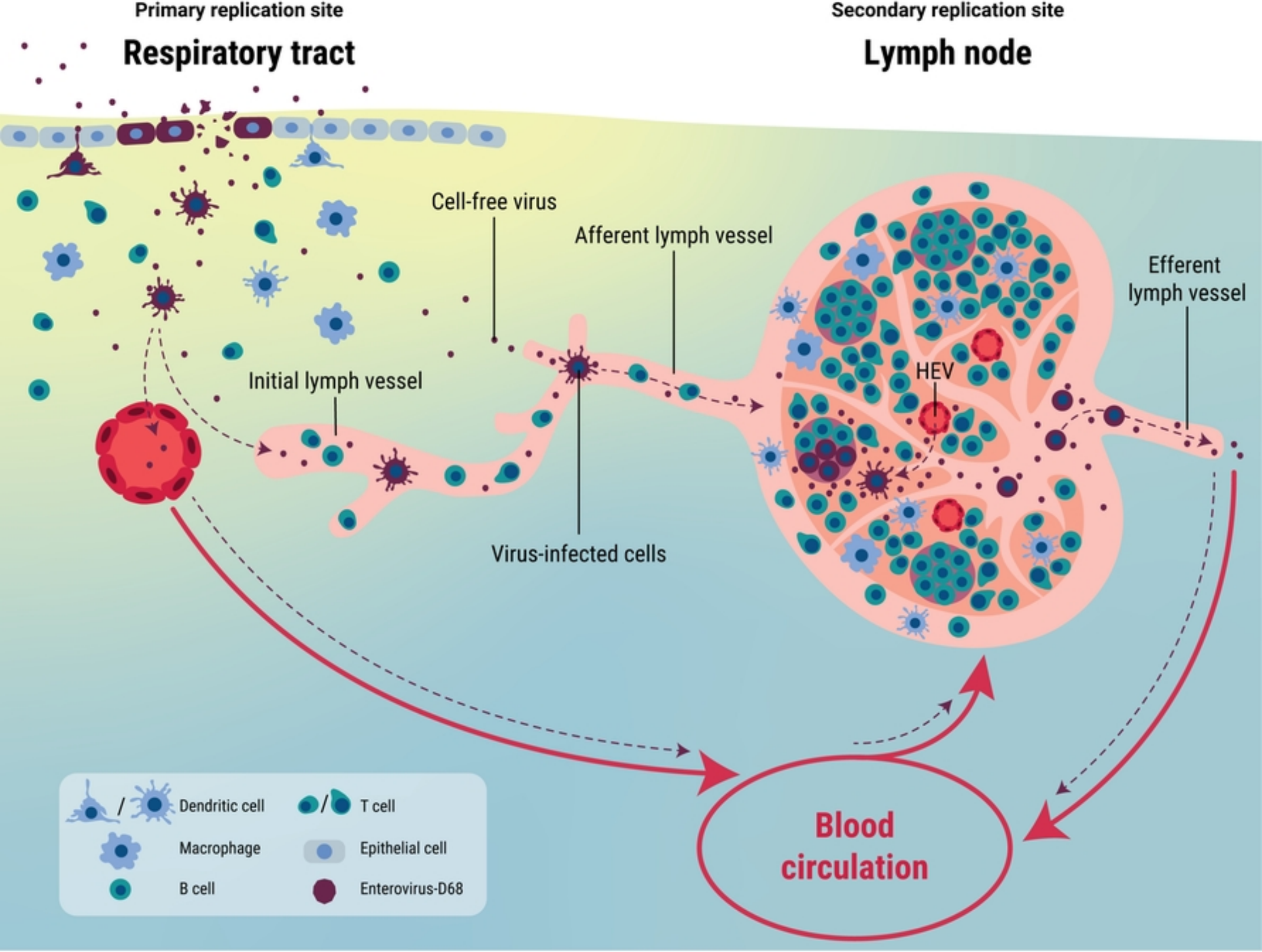
Primary replication site
Respiratory tract
Secondary replication site
Lymph node
Cell-free virus
Afferent lymph vessel
Efferent lymph vessel
Initial lymph vessel
HEV
Virus-infected cells
Blood circulation
Dendritic cell
T cell
Macrophage
Epithelial cell
B cell
Enterovirus-D68

Fig 6